The Hong Kong Polytechnic University

Department of Applied Mathematics

Existence of traveling wave solutions of a hyperbolic system

Zengyan ZHANG

A thesis submitted in partial fulfilment of the requirements

for the degree of Master of Philosophy

June 2017

Certificate of Originality

I hereby declare that this thesis is my own work and that, to the best of my knowledge and belief, it reproduces no material previously published or written, nor material that has been accepted for the award of any other degree or diploma, except where due acknowledgement has been made in the text.

_____(Signed)

_____ ZHANG Zengyan _____(Name of student)

Dedicate to my parents.

Abstract

In thesis, we establish and prove the existence of traveling wave solutions of a hyperbolic system. This system has various applications in many fields, in particular, biological science, such as chemotactic movement of bacteria, aggregation of microglia in Alzheimer's disease, tumor angiogenesis and reinforced random walkers, etc.. One of prominent phenomena is the propagating of traveling waves. Numerical simulations will be represented to illustrate the process of forming steadily wave propagation in those applications. In addition, open problems are proposed for further study.

Acknowledgements

The endeavor of carrying out research is a fascinatingly non-isolated activity. I am grateful to the several individuals who have supported me in various ways during the M.Phil program and would like to hereby acknowledge their assistance.

First and foremost, I wish to express my heartfelt appreciation to my supervisors, Prof. Yanping Lin and Prof. Zhi-an Wang, for their enlightening guidance, invaluable discussions, insightful ideas and great patience throughout these years. What I have benefited most is the rigorous and diligent attitude to scientific research.

Furthermore, I would like to express my deep thanks to my family. Without their strong encouragement and full support, I would not finish my study in Hong Kong.

Finally, I would like to express my special thanks to my friends for their encouragement and support.

x

Contents

Chapter 1

Introduction

1.1 Background

In numerous phenomena, the interesting and fascinating part of a developmental process is the appearance of traveling waves. Traveling wave is a kind of wave, where the shape and speed of propagation of wave are unchanged. For example, after vibrating a stretched rope, it is easy to see that the shape of the wave pulse that travels along the rope is approximately unchanged. Moreover, traveling wave phenomena widely exists in biological systems. Species in this complex environment maintain their own various activities by responding to the internal and external signals and propagating waveforms of various chemical concentrations plays a crucial role in transporting chemical information. There are many examples demonstrating the existence of wave phenomena. For example, the transmission of advantageous genes in a population [7]; branching pattern formation of colonies of the bacteria, *Paenibacillus dendritiformis* [4, 24]; the propagating of calcium waves on the surface of fish eggs during fertilization, like *Medaka* eggs [8], *Sand Dollar* eggs [43], *Zebrafish* eggs [17], etc.; the development of atherosclerosis [5, 18]; the spreading of an epidemic, like *Rabies* ([25],Chpater 13), and so on. In the past several decades, mathematical modeling is an important tool for theoretical analysis of those processes. In 1937, the famous Fisher equation in one dimensional space was developed as a reaction-diffusion mod-

el in [7] to describe the "motion" of advantageous genes and it is a fundamental model from which many variations were developed to analyze the migration of single species.

In addition to simple combination of reaction and diffusion mechanism, chemotaxis is also a key factor needs to be considered in the formation of traveling wave patterns. Chemotaxis represents an oriented movement of bacteria or cellular organisms influenced by the concentration gradient of the chemical, such as the aggregation of cellular slime molds *Dictyosteilum discoideum* into a number of centers which is stimulated by a chemical substance, *cyclic AMP* [12, 39]. Another well-known example is the migration of *Escherichia coli* (*E.coli*) towards oxygen. J. Adler (1965) [1, 2] conducted experiments to illustrate how bacteria react to the chemotactic attractants and repellents. In the experiments, there is a closed capillary tube filled with oxygen and energy source, and a sharp traveling band of bacteria was observed shortly after *E.coli* was placed at one end of the tube. Later, in 1970s, Keller and Segel formulated a well-known chemotaxis model [13, 14] whose general form is,

$$
\begin{cases}
u_t = \nabla \cdot (du_x - \chi u \nabla \phi(h)), \\
h_t = \varepsilon \Delta h + f(u, h).
\end{cases}
\tag{1.1}
$$

where $u(x, t)$ and $h(x, t)$ denote the density of bacteria and the concentration of chemical substrate respectively. $d > 0$ is the diffusion coefficient of bacteria which measures cellular motility. $\varepsilon \geq 0$ is the diffusion rate of the chemical substrate. The attractive strength of the chemical signal is represented by chemotactic coefficient, χ, with $\chi > 0$ which means the chemical is a kind of chemotactic attractant. $f(u, h)$ is a function describing the chemical production and degradation induced by the consumption effect of cells. The chemosensitivity function, $\phi(h)$, demonstrates how level of chemical concentration influence cellular sensitivity. The original Keller-Segel model considers the logarithmic sensitivity which is $\phi(h) = \ln h$. Also, there

2

are other typical forms of function, such as, $\phi(h) = kh$ (linear law) [10, 3] and
$\phi(h) = kh^m/(1 + h^m)$ (receptor law) with $k > 0$ and $m \in \mathbb{N}$, see [32, 34, 38].

Here we review the existence of traveling wave solutions of Keller-Segel model in one dimensional space with logarithmic law, $\phi(h) = \ln h$ and $f(u, h) = \beta h - ug(h)$, where β is the growth rate if $\beta > 0$ or the degradation rate if $\beta < 0$.

$$
\begin{aligned}
u_t &= (du_x - \chi u h^{-1} h_x)_x, \\
h_t &= \varepsilon h_{xx} + \beta h - ug(h).
\end{aligned}
\tag{1.2}
$$

In addition, $g(h)$ is the consumption rate of the chemical per cell with the following different forms represented in [41].

$$
g(h) = h^m =
\begin{cases}
\text{constant rate} & m = 0, \\
\text{sublinear rate} & 0 < m < 1, \\
\text{linear rate} & m = 1, \\
\text{superlinear rate} & m > 1.
\end{cases}
$$

There are many other properties of Keller-Segel model, such as, linear and nonlinear stability, global existence and asymptotic decay rates, etc., please refer to [9, 10, 41] and references therein. When $\beta < 0$, non-existence of traveling wave solution was proved in [41]. Moreover, when $\beta \geq 0$, results referring to the existence of traveling wave solutions will be sketched below.

Substituting the traveling wave ansatz $(u, h)(x, t) = (U, H)(z)$ with $z = x - ct$ into the system (1.2) and integrating it gives

$$
\begin{cases}
dU' + cU - \chi H^{-1} H' U = C_0, \\
\varepsilon H'' + cH' - UH^m + \beta H = 0
\end{cases}
$$

where c is the wave speed, $c \geq 0$, and C_0 is an integration constant.

For the case of zero integration constant ($C_0 = 0$), under the condition $\varepsilon = 0$, when $0 \leq m < 1$ and $\beta = 0$, system (1.2) is the original Keller-Segel model and traveling wave solutions were explicitly found in [14, 27, 11, 31, 30, 15, 28]; when $0 \leq m < 1$

and $\beta > 0$, the existence of traveling wave solutions was established in [41]; when $m = 1$, the existence of traveling wave solutions were derived in [42, 19, 40]; On the other hand, under the condition $\varepsilon > 0$, wonderful results concerning traveling wave solutions were established by a change of independent variable in [26] for $m = 0$, $\beta = 0$ and $d > \chi$. With regard to other numerous results and rigorous proofs of existence of traveling wave solutions, please refer to [23, 41].

For the case of non-zero integration constant $(C_0 \neq 0)$, there are many open problems remain to be solved. Nevertheless, when $m = 1$, $\varepsilon \geq 0$, there are rigorous results showed in [42, 19, 20, 21]. Considering the singularity caused by H^{-1} as $H \to 0$ and the difficulty for solving ODE system by introducing a new variable to replace H'' when $\varepsilon > 0$, the following Hopf-Cole type transformation was applied to system (1.2) in [42].

$$v = -\frac{h_x}{h} = -(\ln h)_x$$

The transformation yields the following system of conservation laws

$$\begin{cases} u_t - \chi(uv)_x = du_{xx}, \\ v_t + (\varepsilon v^2 - u)_x = \varepsilon v_{xx} \end{cases} \tag{1.3}$$

In this thesis, we study the existence of traveling wave solutions of the following system

$$\begin{cases} u_t - \chi(uv)_x = du_{xx}, \\ v_t - (\sigma v^2 + u)_x = \varepsilon v_{xx} \end{cases} \tag{1.4}$$

with ε, $d \geq 0$ and $\sigma \in \mathbb{R}$. System (1.3) is the special case of our model with $\sigma = -\varepsilon$ and $\alpha = 1$. By assigning different values to those parameters, it has many other variations and applications which will be introduced in next section.

1.2 The model variations and applications

Attraction-repulsion chemotaxis model

As $d > 0$, $\varepsilon > 0$, $\sigma = 0$, the system (1.4) becomes a particular case of the following attraction-repulsion chemotaxis model:

$$
\begin{cases}
u_t = d\Delta u - \nabla \cdot (\chi u \nabla s) + \nabla \cdot (\xi u \nabla w), \\
s_t = \varepsilon \Delta s + \alpha u - \beta s, \\
w_t = \varepsilon \Delta w + \gamma u - \delta w.
\end{cases}
\tag{1.5}
$$

This model was proposed in [22] to describe the process of aggregation of *Microglia* (denoted by u) due to the interaction with chemical substances, chemoattractant, β-amyloid (denoted by s) and chemorepellent, Tumor necrosis factor (TNF-α) (denoted by w). It is a chemotaxis system where the distribution of diffusible signaling chemicals (β-amyloid and TNF-α) affects the spacing of cells while the production of chemicals are induced by motile cells. In [22], χ, ξ, β, $\delta \geqslant 0$, α, $\gamma > 0$ are parameters. When $\beta = \delta = 0$, our model (1.4) with $\sigma = 0$ can be derived from the system (1.5) by setting $v = \xi \nabla w - \chi \nabla s$ and $\theta = \xi \gamma - \alpha \chi$.

Initation of capillary formation in tumor angiogenesis

As $\sigma = -\varepsilon$ and $d > 0$, then the system (1.4) is a system transformed from a chemotaxis system proposed in [18], which is

$$
\begin{cases}
u_t = d\Delta u - \nabla \cdot (\chi u \nabla \ln w), \\
w_t = \varepsilon \Delta w - uw.
\end{cases}
\tag{1.6}
$$

with $\chi > 0$. This model is intended to describe the formation of new blood vessels, capillaries, during the growth of tumor. Moreover, the smallness of ε is emphasized in [18] which means the diffusivity of chemicals could be negligible (i.e. $0 \leqslant \varepsilon \ll 1$) because the interactions between molecules are far more important after the onset of tumor angiogenesis. The system (1.6) becomes our model (1.4) with $\sigma = -\varepsilon$ by

the following Cole-Hopf type transformation.

$$v = -\nabla \ln w = -\frac{\nabla w}{w}$$

Repulsive chemotaxis system with logarithmic sensitivity

As $\sigma = \varepsilon$ and $d > 0$, the following system is a repulsive chemotaxis system with logarithmic sensitivity which is

$$\begin{cases} u_t = d\Delta u - \nabla \cdot (\chi u \nabla \ln w), \\ w_t = \varepsilon \Delta w + uw - \mu w. \end{cases} \tag{1.7}$$

In many theoretical analysis of chemotaxis, the signal is transported by diffusion and convection. However, this system derived in [35, 36] is modeled by reinforced random walkers (denoted by u), such as *myxobacteria*. The signals (denoted by w) released by cells can modify the local environment in a strictly local manner for succeeding passages $\chi > 0$ and there is little or no transport (i.e. $0 \leqslant \varepsilon \ll 1$ is small) of the modifying substance (denoted by w). Similarly, under the situation $\sigma = \varepsilon = 0$, our model can be derived from (1.7) by Cole-Hopf type transformation $v = \nabla \ln w = \frac{\nabla w}{w}$.

Except aforementioned applications in chemotaxis, the model (1.4) has applications in fluid dynamics. For example, when $d = \varepsilon = 0$ and $\sigma = -1$, the system (1.4) is the LeRoux system of conservation law, see [33]. Hence (1.4) can be regarded as the viscous LeRoux system. Another application in fluid dynamics is the following Boussineq-Burger system.

Boussineq-Burger system without dispersion

As $\sigma = \frac{1}{2}$, $w = -v$, the following Boussineq-Burger system without dispersion term model describes the bore formation in shall water propagation considered in [29]. Furthermore, in [29], the author studied the existence of traveling wave solutions of

system (1.8).

$$\begin{cases} u_t + (uw)_x = du_{xx}, \\ \\ w_t + (u + \dfrac{w^2}{2})_x = \varepsilon w_{xx} + \delta w_{xxt}. \end{cases} \tag{1.8}$$

However, our theoretical analysis and numerical simulations are mainly focus on the applications in biological systems.

1.3 Organization of the Thesis

In Chapter 2, we introduce some definitions and theorems which will be used in the following chapters. Then we state the main result and show the existence of traveling wave solutions of the model (1.4) in Chapter 3. Also, numerical simulation results are represented in Chapter 4. Finally, Chapter 5 concludes the whole thesis and open problems in related fields.

Chapter 2

Preliminary

In this chapter, we will review some concepts and present the theorem which will be used in the following chapters.

Considering the following system of conservation laws in one space dimension.

$$\mathbf{u}_t + \mathbf{F}(\mathbf{u})_x = 0 \quad \text{in} \ \ \mathbb{R} \times (0, \infty) \tag{2.1}$$

where $\mathbf{F} : \mathbb{R}^m \to \mathbb{R}^m$ and $\mathbf{u} : \mathbb{R} \times [0, \infty) \to \mathbb{R}^m$ is the unknown, $\mathbf{u} = \mathbf{u}(x, t)$. And the nondivergence form of (2.1) is

$$\mathbf{u}_t + \mathbf{B}(\mathbf{u})\mathbf{u}_x = 0 \quad \text{in} \ \ \mathbb{R} \times (0, \infty) \tag{2.2}$$

where $\mathbf{B} : \mathbb{R}^m \to \mathbb{M}^{m \times m}$ and $\mathbf{B} = D\mathbf{F}$.

In the section 3.1, we will use the following definitions introduced in [6] to check the hyperbolicity of system (1.4) and make sure $(\lambda_k, \boldsymbol{\gamma}_k)$ is genuinely nonlinear for the purpose of finding traveling wave solutions.

Definition 2.1. *If for each $w \in \mathbb{R}^m$ the eigenvalues of $\mathbf{B}(w)$ are real and distinct, then the system (2.2) is strictly hyperbolic.*

Definition 2.2. *The pair $(\lambda_k(w), \boldsymbol{\gamma}_k(w))$ is called genuinely nonlinear provided*

$$D\lambda_k(w) \cdot \boldsymbol{\gamma}_k(w) \neq 0 \quad \text{for all } w \in \mathbb{R}^m.$$

where $\lambda_k(w)$ $(k = 1, \ldots m)$ denote the real and distinct eigenvalues of $\boldsymbol{B}(w)$ and $\boldsymbol{\gamma}_k(w)$ $(k = 1, \ldots m)$ denote a corresponding nonzero eigenvector.

Then under the condition that $(\lambda_k, \boldsymbol{\gamma}_k)$ is genuinely nonlinear, we use the following Lax's entropy condition [37] as the entropy criteria for admissible shock waves.

$$\lambda_k(u_r) < c(u_r, u_l) < \lambda_k(u_l).$$

where u_l and u_r are the left and right initial states.

Furthermore, we use the following Poincaré Bendixson theorem [37] for the proof of the existence of traveling wave solutions.

Theorem 2.1 (Generalized Poincaré Bendixson theorem). *Let M be an open subset of $\mathbb{R}^2$ and $f \in C^1(M, \mathbb{R}^2)$. Fix $x \in M$, $\sigma \in \{\pm\}$, and suppose $\omega_\sigma(x) \neq \emptyset$ is compact, connected, and contains only finitely many fixed points. Then one of the following cases holds:*

(i) $\omega_\sigma(x)$ is a fixed orbit.,

(ii) $\omega_\sigma(x)$ is a regular periodic orbit.

(iii) $\omega_\sigma(x)$ consists of (finitely many) fixed points $\{x_j\}$ and non-closed orbits $\gamma(y)$ such that $\omega_\pm(y) \in \{x_j\}$.

Chapter 3

Existence of traveling wave solutions

In this chapter, we discuss the existence of the traveling wave solutions of the following system (1.4),

$$
\begin{cases}
u_t - \chi(uv)_x = du_{xx}, \\
v_t - (\sigma v^2 + u)_x = \varepsilon v_{xx}.
\end{cases}
$$

3.1 Existence of the traveling wave solutions

First, we substitute the following scalings into (1.4)

$$
\tilde{v} = \sqrt{\chi}v, \quad \tilde{x} = \sqrt{\frac{1}{\chi}}x, \quad \tilde{d} = \frac{d}{\chi}, \quad \tilde{\varepsilon} = \frac{\varepsilon}{\chi}, \quad \tilde{\sigma} = \frac{\sigma}{\chi}.
$$

and drop the tildes for simplification, then we obtain the following system

$$
\begin{cases}
u_t - (uv)_x = du_{xx}, \\
v_t - (\sigma v^2 + u)_x = \varepsilon v_{xx}.
\end{cases}
\tag{3.1}
$$

In the absence of viscosity and under some conditions for σ, we shall show that the system (3.1) is a genuinely nonlinear hyperbolic system.

Without the viscous term, the system (3.1) becomes

$$
\begin{cases}
u_t - (uv)_x = 0, \\
v_t - (\sigma v^2 + u)_x = 0.
\end{cases}
\tag{3.2}
$$

The Jacobian matrix of system (3.2) is

$$J(u,v) = \begin{bmatrix} -v & -u \\ -1 & -2\sigma v \end{bmatrix}$$

and its eigenvalues satisfy

$$\lambda^2 + (2\sigma + 1)v\lambda + 2\sigma v^2 - u = 0 \tag{3.3}$$

which has two real roots

$$\begin{aligned}
\lambda_1(u,v) &= -\frac{(2\sigma+1)v}{2} - \frac{\sqrt{(2\sigma-1)^2 v^2 + 4u}}{2} \\
\lambda_2(u,v) &= -\frac{(2\sigma+1)v}{2} + \frac{\sqrt{(2\sigma-1)^2 v^2 + 4u}}{2}
\end{aligned} \tag{3.4}$$

with respective eigenvectors

$$\Phi_1(u,v) = \begin{bmatrix} -\lambda_1 - 2\sigma v \\ 1 \end{bmatrix}, \qquad \Phi_2(u,v) = \begin{bmatrix} \lambda_2 + 2\sigma v \\ -1 \end{bmatrix}$$

Because $u \geq 0$, then λ_1 and λ_2 are two real and distinct eigenvalues with $\lambda_1 < \lambda_2$.

Hence, system (3.2) is hyperbolic.

Furthermore, we have from straightforward calculations that

$$\begin{aligned}
\nabla\lambda_1(u,v) \cdot \Phi_1(u,v) &= -1 - \frac{v}{\sqrt{(2\sigma-1)^2 v^2 + 4u}} - \sigma - \frac{\sigma(2\sigma-3)v}{\sqrt{(2\sigma-1)^2 v^2 + 4u}} \\
&= -1 - \sigma - \frac{(2\sigma-1)(\sigma-1)v}{\sqrt{(2\sigma-1)^2 v^2 + 4u}} \\
\nabla\lambda_1(u,v) \cdot \Phi_2(u,v) &= 1 - \frac{v}{\sqrt{(2\sigma-1)^2 v^2 + 4u}} + \sigma - \frac{\sigma(2\sigma-3)v}{\sqrt{(2\sigma-1)^2 v^2 + 4u}} \\
&= 1 + \sigma - \frac{(2\sigma-1)(\sigma-1)v}{\sqrt{(2\sigma-1)^2 v^2 + 4u}}
\end{aligned}$$

12

We consider $\nabla\lambda_1(u,v) \cdot \Phi_1(u,v) < 0$ and $\nabla\lambda_2(u,v) \cdot \Phi_2(u,v) > 0$ to ensure that the hyperbolic system (3.2) is genuinely nonlinear.

$\nabla\lambda_1(u,v) \cdot \Phi_1(u,v) < 0$ and $\nabla\lambda_2(u,v) \cdot \Phi_2(u,v) > 0$ show that

$$\begin{cases} -(1+\sigma) < \dfrac{(2\sigma-1)(\sigma-1)v}{\sqrt{(2\sigma-1)^2 v^2 + 4u}} \\[4mm] (1+\sigma) > \dfrac{(2\sigma-1)(\sigma-1)v}{\sqrt{(2\sigma-1)^2 v^2 + 4u}} \end{cases} \tag{3.5}$$

We can see from (3.5) that $1 + \sigma > 0$ which means $\sigma > -1$. Then we divide it into four cases to discuss the conditions for σ.

Case i. When $v > 0$ and $(2\sigma-1)(\sigma-1) < 0$ which is $\frac{1}{2} < \sigma < 1$, we only need to consider

$$-(1+\sigma) < \frac{(2\sigma-1)(\sigma-1)v}{\sqrt{(2\sigma-1)^2 v^2 + 4u}}$$

$$\Longleftrightarrow \qquad (1+\sigma)^2 > \frac{(2\sigma-1)^2(\sigma-1)^2 v^2}{(2\sigma-1)^2 v^2 + 4u}$$

$$\Longleftrightarrow \qquad 4u(\sigma+1)^2 > v^2(2\sigma-1)^2(-4\sigma)$$

Because $\frac{1}{2} < \sigma < 1$ and $u > 0$, then it always holds.

Case ii. When $\sigma > -1$, $v > 0$ and $(2\sigma-1)(\sigma-1) > 0$ which is $-1 < \sigma < \frac{1}{2}$ or $\sigma > 1$, we only need to consider

$$(1+\sigma) > \frac{(2\sigma-1)(\sigma-1)v}{\sqrt{(2\sigma-1)^2 v^2 + 4u}}$$

13

If $0 < \sigma < \frac{1}{2}$ or $\sigma > 1$, it is easy to see that it always holds.

If $-1 < \sigma < 0$, we consider

$$1 - \frac{v}{\sqrt{(2\sigma-1)^2 v^2 + 4u}} > -\sigma + \frac{\sigma(2\sigma-3)v}{\sqrt{(2\sigma-1)^2 v^2 + 4u}}$$

$$\Longleftrightarrow \quad 1 - \frac{v}{\sqrt{(2\sigma-1)^2 v^2 + 4u}} > -\sigma\left(1 - \frac{(2\sigma-3)v}{\sqrt{(2\sigma-1)^2 v^2 + 4u}}\right)$$

$$\Longleftrightarrow \quad -\sigma < \frac{1 - \frac{v}{\sqrt{(2\sigma-1)^2 v^2 + 4u}}}{1 - \frac{(2\sigma-3)v}{\sqrt{(2\sigma-1)^2 v^2 + 4u}}}$$

$$\Longleftrightarrow \quad \sigma > -\frac{1 - \frac{v}{\sqrt{(2\sigma-1)^2 v^2 + 4u}}}{1 - \frac{(2\sigma-3)v}{\sqrt{(2\sigma-1)^2 v^2 + 4u}}} > -1$$

Then for $v > 0$, we require

$$\sigma > -\frac{1 - \frac{v}{\sqrt{(2\sigma-1)^2 v^2 + 4u}}}{1 - \frac{(2\sigma-3)v}{\sqrt{(2\sigma-1)^2 v^2 + 4u}}}, \quad \text{with } 0 < \frac{1 - \frac{v}{\sqrt{(2\sigma-1)^2 v^2 + 4u}}}{1 - \frac{(2\sigma-3)v}{\sqrt{(2\sigma-1)^2 v^2 + 4u}}} < 1$$

Case iii, when $v < 0$ and $(2\sigma - 1)(\sigma - 1) < 0$ which is $\frac{1}{2} < \sigma < 1$, we only need to consider

$$(1 + \sigma) > \frac{(2\sigma - 1)(\sigma - 1)v}{\sqrt{(2\sigma - 1)^2 v^2 + 4u}}$$

We know it always holds when $\frac{1}{2} < \sigma < 1$.

Case iv, when $\sigma > -1$, $v < 0$ and $(2\sigma - 1)(\sigma - 1) > 0$ which is $-1 < \sigma < \frac{1}{2}$ or $\sigma > 1$, we only need to consider

$$-(1 + \sigma) < \frac{(2\sigma - 1)(\sigma - 1)v}{\sqrt{(2\sigma - 1)^2 v^2 + 4u}}$$

It is easy to see that it always holds for $0 < \sigma < \frac{1}{2}$ or $\sigma > 1$.

If $-1 < \sigma < 0$, we consider

$$-1 - \frac{v}{\sqrt{(2\sigma - 1)^2 v^2 + 4u}} < \sigma + \frac{\sigma(2\sigma - 3)v}{\sqrt{(2\sigma - 1)^2 v^2 + 4u}}$$

$$\Longleftrightarrow \quad -(1 + \frac{v}{\sqrt{(2\sigma - 1)^2 v^2 + 4u}}) < \sigma(1 + \frac{(2\sigma - 3)v}{\sqrt{(2\sigma - 1)^2 v^2 + 4u}})$$

$$\Longleftrightarrow \qquad\qquad \sigma > -\frac{1 + \frac{v}{\sqrt{(2\sigma-1)^2 v^2 + 4u}}}{1 + \frac{(2\sigma-3)v}{\sqrt{(2\sigma-1)^2 v^2 + 4u}}} > -1$$

Then for $v < 0$, we require

$$\sigma > -\frac{1 + \frac{v}{\sqrt{(2\sigma-1)^2 v^2 + 4u}}}{1 + \frac{(2\sigma-3)v}{\sqrt{(2\sigma-1)^2 v^2 + 4u}}}, \quad \text{with } 0 < \frac{1 + \frac{v}{\sqrt{(2\sigma-1)^2 v^2 + 4u}}}{1 + \frac{(2\sigma-3)v}{\sqrt{(2\sigma-1)^2 v^2 + 4u}}} < 1$$

In summary, we show that if

$$\sigma > \sigma_0 = -\frac{1 - \frac{|v|}{\sqrt{(2\sigma-1)^2 v^2 + 4u}}}{1 - \frac{(2\sigma-3)|v|}{\sqrt{(2\sigma-1)^2 v^2 + 4u}}}, \quad \text{with } 0 < \sigma_0 < 1 \qquad (3.6)$$

the hyperbolic system (3.2) is genuinely nonlinear.

Moreover, according to the definition of hyperbolicity in Chapter 2, we also consider other three different cases, and the results are listed in table 3.1.

Next we define the following traveling wave ansatz

$$(u, v)(x, t) = (U, V)(z), \quad z = x - ct$$

where z denotes the traveling wave variable and c represents the wave speed.

Table 3.1: Other three different cases

	$v > 0$	$v < 0$
$\nabla\lambda_1(u,v)\cdot\Phi_1(u,v) > 0$ and $\nabla\lambda_2(u,v)\cdot\Phi_2(u,v) < 0$	If $1 - \frac{u}{2v^2} > -1$, then it is not true. If $1 - \frac{u}{2v^2} < -1$, then $1 - \frac{u}{2v^2} < \sigma < -\dfrac{1+\frac{v}{\sqrt{(2\sigma-1)^2v^2+4u}}}{1+\frac{(2\sigma-3)v}{\sqrt{(2\sigma-1)^2v^2+4u}}}$	If $1 - \frac{u}{2v^2} > -1$, then it is not true. If $1 - \frac{u}{2v^2} < -1$, then $1 - \frac{u}{2v^2} < \sigma < -\dfrac{1-\frac{v}{\sqrt{(2\sigma-1)^2v^2+4u}}}{1-\frac{(2\sigma-3)v}{\sqrt{(2\sigma-1)^2v^2+4u}}}$
$\nabla\lambda_1(u,v)\cdot\Phi_1(u,v) > 0$ and $\nabla\lambda_2(u,v)\cdot\Phi_2(u,v) > 0$	It is not true.	If $1 - \frac{u}{2v^2} > -1$, $\sigma < -\dfrac{1+\frac{v}{\sqrt{(2\sigma-1)^2v^2+4u}}}{1+\frac{(2\sigma-3)v}{\sqrt{(2\sigma-1)^2v^2+4u}}}$. If $1 - \frac{u}{2v^2} < -1$, then $\max\{1 - \frac{u}{2v^2}, -\dfrac{1-\frac{v}{\sqrt{(2\sigma-1)^2v^2+4u}}}{1-\frac{(2\sigma-3)v}{\sqrt{(2\sigma-1)^2v^2+4u}}}\} < \sigma < -\dfrac{1+\frac{v}{\sqrt{(2\sigma-1)^2v^2+4u}}}{1+\frac{(2\sigma-3)v}{\sqrt{(2\sigma-1)^2v^2+4u}}}$
$\nabla\lambda_1(u,v)\cdot\Phi_1(u,v) < 0$ and $\nabla\lambda_2(u,v)\cdot\Phi_2(u,v) < 0$	If $1 - \frac{u}{2v^2} > -1$, $\sigma < -\dfrac{1-\frac{v}{\sqrt{(2\sigma-1)^2v^2+4u}}}{1-\frac{(2\sigma-3)v}{\sqrt{(2\sigma-1)^2v^2+4u}}}$. If $1 - \frac{u}{2v^2} < -1$, then $\max\{1 - \frac{u}{2v^2}, -\dfrac{1+\frac{v}{\sqrt{(2\sigma-1)^2v^2+4u}}}{1+\frac{(2\sigma-3)v}{\sqrt{(2\sigma-1)^2v^2+4u}}}\} < \sigma < -\dfrac{1-\frac{v}{\sqrt{(2\sigma-1)^2v^2+4u}}}{1-\frac{(2\sigma-3)v}{\sqrt{(2\sigma-1)^2v^2+4u}}}$	It is not true.

Substituting the above traveling wave ansatz into (3.1), one yields the following traveling wave equations

$$\begin{cases} -cU_z - (UV)_z = dU_{zz}, \\ -cV_z - (\sigma V^2 + U)_z = \varepsilon V_{zz}. \end{cases} \tag{3.7}$$

with boundary conditions

$$(U,V)(z) \to (u_\pm, v_\pm) \quad \text{as } z \to \pm\infty \tag{3.8}$$

where $u_\pm \geqslant 0$.

Integrating (3.7) and we can obtain the following ODE system

$$\begin{cases} dU_z = -cU - UV + \rho_1 =: F(U,V) \\ \varepsilon V_z = -cV - \sigma V^2 - U + \rho_2 =: G(U,V) \end{cases} \tag{3.9}$$

16

where ρ_1, ρ_2 are constants that satisfy

$$\rho_1 = cu_- + u_- v_- = cu_+ + u_+ v_+,$$
$$\rho_2 = cv_- + \sigma v_-^2 + u_- = cv_+ + \sigma v_+^2 + u_+. \tag{3.10}$$

Rearranging (3.10), from direct calculations, the wave speed c is determined by

$$\begin{cases} c(u_+ - u_-) + (u_+ v_+ - u_- v_-) = 0 \\ c(v_+ - v_-) + \left(\sigma(v_+^2 - v_-^2) + u_+ - u_-\right) = 0 \end{cases} \tag{3.11}$$

from which we can deduce a quadratic equation of wave speed c.

$$c^2 + v_- c + u_+ \left(\frac{-\sigma(v_+^2 - v_-^2)}{u_+ - u_-} - 1\right) = 0 \tag{3.12}$$

Note that when σ satisfies

$$\frac{-\sigma(v_+^2 - v_-^2)}{u_+ - u_-} < 1, \tag{3.13}$$

then the discriminant of the quadratic equation (3.12) is positive. Therefore (3.12) has two solutions. The positive solution gives the wave speed of the second characteristic family of system (3.1) while the negative solution gives the wave speed of the first characteristic family. Hereforth we only take the case $c > 0$ into account and the analysis can be extended to the case $c < 0$. The positive wave speed c is given by

$$c = -\frac{v_-}{2} + \frac{1}{2}\sqrt{v_-^2 + 4u_+\left(1 + \frac{\sigma(v_+^2 - v_-^2)}{u_+ - u_-}\right)} \tag{3.14}$$

Then if $v_- > 0$, $c + v_- \geq 0$ always holds. And if $v_- \leq 0$ and $\frac{-\sigma(v_+^2 - v_-^2)}{u_+ - u_-} - 1 < 0$, then $c \geq |v_-| = -v_-$, which is equivalent to

$$c + v_- \geq 0 \tag{3.15}$$

The entropy condition for the shock of second characteristic family (e.g. see [16]) is

$$\lambda_2(u_+, v_+) < c < \lambda_2(u_-, v_-) \tag{3.16}$$

where $\lambda_2(u, v)$ is defined in (3.4). When σ is small, we derive form the entropy inequality (3.16) that

Indeed $c < \lambda_2(u_-, v_-)$ first gives,

$$-\frac{(2\sigma + 1)v_-}{2} + \frac{\sqrt{(2\sigma - 1)^2 + 4u_-}}{2} > -\frac{v_-}{2} + \frac{1}{2}\sqrt{v_-^2 + 4u_+(1 + \frac{\sigma(v_+^2 - v_-^2)}{u_+ - u_-})}$$

$$\Longleftrightarrow \quad -\frac{v_-}{2} + \frac{\sqrt{v_-^2 + 4u_-}}{2} > -\frac{v_-}{2} + \frac{\sqrt{v_-^2 + 4u_+}}{2}$$

$$\Longleftrightarrow \quad u_- > u_+$$

On the other hand, $\lambda_2(u_+, v_+) < c$ gives,

$$-\frac{(2\sigma + 1)v_+}{2} + \frac{\sqrt{(2\sigma - 1)^2 + 4u_+}}{2} < -\frac{v_-}{2} + \frac{1}{2}\sqrt{v_-^2 + 4u_+(1 + \frac{\sigma(v_+^2 - v_-^2)}{u_+ - u_-})}$$

$$\Longleftrightarrow \quad -\frac{v_+}{2} + \frac{\sqrt{v_+^2 + 4u_+}}{2} < -\frac{v_-}{2} + \frac{\sqrt{v_-^2 + 4u_+}}{2}$$

$$\Longleftrightarrow \quad \frac{v_- - v_+}{2} < \frac{\sqrt{v_-^2 + 4u_+} - \sqrt{v_+^2 + 4u_+}}{2}$$

$$\Longleftrightarrow \quad v_- - v_+ < \frac{(v_- - v_+)(v_- + v_+)}{\sqrt{v_-^2 + 4u_+} + \sqrt{v_+^2 + 4u_+}}$$

$$\Longleftrightarrow \quad 0 < \left(\frac{v_- + v_+}{\sqrt{v_-^2 + 4u_+} + \sqrt{v_+^2 + 4u_+}} - 1\right)(v_- - v_+)$$

$$\Longleftrightarrow \quad v_- < v_+$$

In summary, from the entropy inequality (3.16), we can have

$$0 \leq u_+ < u_-, \quad v_- < v_+ \tag{3.17}$$

18

which will be used in phase-plane analysis.

Now we can conclude the following result concerning the existence of traveling wave solutions of (3.1), namely, the existence of solutions to (3.7), (3.8).

Theorem 3.1. *Let the entropy condition (3.16) holds.*

(i) When $\rho_1 = 0$, if $\frac{u_-}{v_-(v_+ - v_-)} < \sigma(\frac{v_+}{v_-} + 1) < 1$ and $\sigma\frac{v_+}{v_-} < \frac{1}{2}$, there exists a monotone shock profile $(U, V)(x - ct)$ to system (3.7), (3.8), which is unique up to a translation and satisfies $U_z < 0$ and $V_z > 0$, where the wave speed $c = -v_-$.

(ii) When $\rho_1 \neq 0$, if $\sigma(v_+ + v_-) < \frac{u_- - u_+}{v_+ - v_-}$ and $\sigma(v_+ + v_-) + (\frac{1}{2} + \sigma)c > 0$, there exists a monotone shock profile $(U, V)(x - ct)$ to system (3.7), (3.8), which is unique up to a translation and satisfies $U_z < 0$ and $V_z > 0$, where the wave speed c is given by (3.14).

3.2   Phase-plane analysis

In this section, we shall use the phase plane analysis to perform the existence of traveling wave solutions of (3.1) as stated in Theorem 3.1. According to the definition of constants ρ_1 and ρ_2 in (3.10), we see that the ODE system (3.9) must have two equilibria (u_-, v_-) and (u_+, v_+) and the number of critical points is presented in the following Table 3.2.

Table 3.2: Number of critical points

	$\rho_1 = 0$	$\rho_1 \neq 0$
$\sigma > 0$	3 $(u_+, v_+), (u_-, v_-),$ $(0, m) = (0, -\frac{c}{\sigma} - v_+)$	2 $(u_+, v_+), (u_-, v_-)$
$\sigma = 0$	2 $(u_+, v_+), (u_-, v_-)$	2 $(u_+, v_+), (u_-, v_-)$
$\sigma < 0$	3 $(u_+, v_+), (u_-, v_-),$ $(0, m) = (0, -\frac{c}{\sigma} - v_+)$	3 $(u_+, v_+), (u_-, v_-),$ $(p, q) = (-\frac{\sigma \rho_1}{c + \sigma v_+ + \sigma v_-}, -\frac{c(\sigma+1)}{\sigma} - v_+ - v_-)$

Next, we examine the properties of critical points in each case. The Jacobian matrix of the linearized system of (3.9) at critical point (u_*, v_*) is

$$\hat{J}(u_*, v_*) = \begin{bmatrix} \frac{-(c+v_*)}{d} & -\frac{u_*}{d} \\ -\frac{1}{\varepsilon} & -\frac{c+2\sigma v_*}{\varepsilon} \end{bmatrix}$$

with eigenvalues γ which satisfy

$$\gamma^2 + \left(\frac{c + v_*}{d} + \frac{c + 2\sigma v_*}{\varepsilon}\right)\gamma + \frac{1}{d\varepsilon}\left((c + v_*)(c + 2\sigma v_*) - u_*\right) = 0 \tag{3.18}$$

It's easy to verify that the discriminant of quadratic equation (3.18) is non-negative in the region $\mathcal{X}$ defined as $\mathcal{X} = \{(u, v) \mid u \geq 0,\ u_* \geq 0\}$. Hence all roots of (3.18) are real.

The two roots γ_1 and γ_2 satisfy

$$\gamma_1 + \gamma_2\Big|_{(u_*, v_*)} = -\left(\frac{c + v_*}{d} + \frac{c + 2\sigma v_*}{\varepsilon}\right),$$

$$\gamma_1 \gamma_2\Big|_{(u_*, v_*)} = \frac{1}{d\varepsilon}\left(c^2 + (2\sigma + 1)v_* c + 2\sigma v_*^2 - u_*\right) =: \mathcal{H}(c, u_*, v_*).$$

3.2.1 Case of $\rho_1 = 0$

First, from the definition of ρ_1 in 3.10 and 3.17, we know $u_+ = 0$ and $c = -v_-$. On the other hand, $u_- > 0$ and from the definition of ρ_2 in 3.10, we have

$$\sigma\left(\frac{v_+}{v_-} + 1\right) < 1 \tag{3.19}$$

Case 1: $\sigma = 0$.

When $\sigma = 0$, there are only two equilibria (u_+, v_+) and (u_-, v_-). At the critical point (u_+, v_+), we have $\gamma_1 = -\frac{c+v_+}{d} < 0$ and $\gamma_2 = -\frac{c}{\varepsilon} < 0$ and hence (u_+, v_+) is a stable nodal sink. At the critical point (u_-, v_-), we have $\gamma_1 = -\frac{c}{2\varepsilon} - \frac{1}{2}\sqrt{\frac{c^2}{\varepsilon^2} + \frac{4u_-}{\varepsilon d}} < 0$ and $\gamma_2 = -\frac{c}{2\varepsilon} + \frac{1}{2}\sqrt{\frac{c^2}{\varepsilon^2} + \frac{4u_-}{\varepsilon d}} > 0$. Therefore, (u_-, v_-) is a saddle point. Next we shall prove that there is a heteroclinic connection between (u_-, v_-) and (u_+, v_+).

When $\sigma = 0$, we look at the nullclines of system (3.7) which are given by

$$\begin{cases} U(V + c) = 0, \\ U = -cV + \rho_2. \end{cases}$$

The first equation gives two straight lines, $U = 0$ and $V = -c$, and the second equation also gives a straight line (see Figure 3.1). To this end, we shall prove the region $\mathcal{G}$ (see Figure 3.1) enclosed by these two curves contains an invariant region of system (3.9) (3.8), which is defined by

$$\mathcal{G} = \{(U, V) \mid 0 \le U \le -cV + \rho_2, \ V \ge -c\}$$

The region $\mathcal{G}$ is bounded by

$$\Gamma_1 = \{(U, V) \mid V = -c, \ 0 < U < u_-\},$$

$$\Gamma_2 = \{(U, V) \mid U = -cV + \rho_2, \ 0 < U < u_-, \ -c < V < v_+\},$$
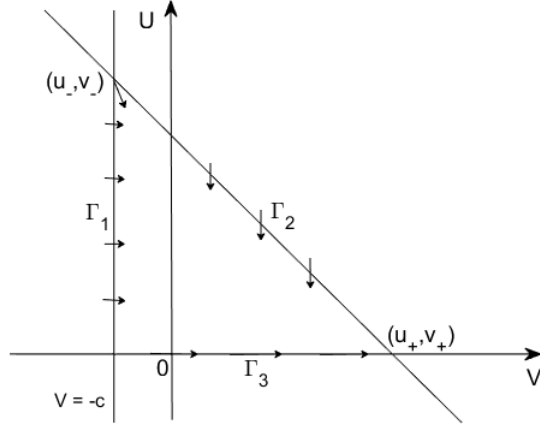
$$\Gamma_3 = \{(U, V) \mid U = 0, \ -c < U < v_+\}.$$

Figure 3.1: Phase portrait for $\rho_1 = 0$ and $\sigma = 0$

Along Γ_1 and Γ_3, we have $U_z = 0$ and the direction field of (3.9) is horizontal. In addition, Γ_1 and Γ_3 are below Γ_2, then we show that $V_z|_{(U,V)\in\Gamma_1,\Gamma_3} > 0$ which means the direction field along the edges Γ_1 and Γ_3 points to the right horizontally. Along the edge Γ_2, we have $V_z = 0$ and the direction field of (3.9) is vertical. Also, from the Figure 3.1, we can see Γ_2 is on the right hand side of Γ_1 and above Γ_3, then it is easy to show that $U_z|_{(U,V)\in\Gamma_2} < 0$ and thus the orbits crossing Γ_2 points downwards. Therefore $\mathcal{G}$ is an invariant region of system (3.9).

Next, we shall prove that the unstable manifold of system (3.9) emanating from the saddle point (u_-, v_-) is trapped inside the invariant region $\mathcal{G}$. From direct calculation, we derive the tangent direction of Γ_1 at (u_-, v_-) is $\frac{dU}{dV}|_{(u_-,v_-)}^{\Gamma_1} = -\infty$ and the tangent direction of Γ_2 at (u_-, v_-) is $\frac{dU}{dV}|_{(u_-,v_-)}^{\Gamma_2} = -c$.

To this end, we compare the direction of the unstable manifold of system (3.9) at the saddle point (u_-, v_-) with the tangent directions of nullclines calculated above. Then we consider the positive eigenvalue of $\hat{J}(u_-, v_-)$ is $\gamma_2 = -\frac{c}{2\varepsilon} + \frac{1}{2}\sqrt{\frac{c^2}{\varepsilon^2} + \frac{4u_-}{\varepsilon d}} > 0$ which has the eigenvector $R_2 = \begin{bmatrix} -\frac{u_-}{d} \\ \gamma_2 \end{bmatrix}$. Hence the slope of the unstable manifold of

22

(3.9) at (u_-, v_-) is

$$\frac{dU}{dV}\Big|_{(u_-,v_-)} = -\frac{c}{2} - \frac{\varepsilon}{2}\sqrt{\frac{c^2}{\varepsilon^2} + \frac{4u_-}{\varepsilon d}}$$

One can easily check that

$$-\infty = \frac{dU}{dV}\Big|_{(u_-,v_-)}^{\Gamma_1} < \frac{dU}{dV}\Big|_{(u_-,v_-)} < \frac{dU}{dV}\Big|_{(u_-,v_-)}^{\Gamma_2} = -c$$

Therefore we deduce that the direction of the unstable manifold of (3.9) at (u_-, v_-)
is between the tangent lines of Γ_2 and Γ_1 at (u_-, v_-) which points inside the region $\mathcal{G}$.
On the basis of the Poincaré-Bendixson theorem, this unstable manifold has to reach
the stable equilibrium (u_+, v_+). This trajectory connecting (u_-, v_-) and (u_+, v_+)
generates a solution for the system (3.9) with $U_z < 0$ and $V_z > 0$.

Case 2: $\sigma \neq 0$

When $\sigma \neq 0$, there are three critical points (u_-, v_-), (u_+, v_+) and $(0, m)$ with $m = -\frac{c}{\sigma} - v_+$.

The nullclines of system (3.7) are

$$\begin{cases} U(V + c) = 0, \\ U = -\sigma V^2 - cV + \rho_2. \end{cases}$$

The first equation gives two straight lines, $U = 0$ and $V = -c$, and the second
equation gives a parabola (see Figure 3.2 for $\sigma < 0$ and Figure 3.3 for $\sigma > 0$).

If σ is small such that

$$\frac{\sigma v_+}{v_-} \leq \frac{1}{2} \tag{3.20}$$

For critical point (u_+, v_+), we have $\gamma_1 = -\frac{c+v_+}{d} < 0$ and $\gamma_2 = -\frac{c+2\sigma v_+}{\varepsilon} < 0$. There-
fore, (u_+, v_+) is a stable nodal sink. From the definition of $\lambda_1(u, v)$ and $\lambda_2(u, v)$ in
(3.4), we have $\lambda_2(u_-, v_-) > c$ for any $\sigma \neq 0$ and $\lambda_1(u_-, v_-) < c$ for any $\sigma \neq 0$.
Therefore, $\lambda_1(u_-, v_-) < c < \lambda_2(u_-, v_-)$ and $\gamma_1\gamma_2|_{(u_-,v_-)} < 0$ which means (u_-, v_-) is

23

a saddle point. For the critical point $(0, m)$, we have two cases to discuss as below. When $\sigma < 0$, the critical point $(0, m)$ with $m > v_+$ is on the right hand side of the symmetry axis of the parabola (see Figure 3.2). Hence, we have $\gamma_1 = -\frac{c+m}{d} < 0$ and $\gamma_2 = -\frac{c+2\sigma m}{\varepsilon} > 0$. Then $(0, m)$ is a saddle point. When $\sigma > 0$, the critical point $(0, m)$ with $m < v_-$ is on the left hand side of the symmetry axis of the parabola (see Figure 3.3). Therefore, we have $\gamma_1 = -\frac{c+m}{d} > 0$ and $\gamma_2 = -\frac{c+2\sigma m}{\varepsilon} > 0$ which means $(0, m)$ is an unstable nodal source. To make a summary, we have the following lemma.

Lemma 3.1. *When $\rho_1 = 0$ and $\sigma \neq 0$, three critical points have the following properties:*

(i) The critical point (u_+, v_+) is a stable nodal sink;

(ii) The critical point (u_-, v_-) is a saddle point;

(iii) When $\sigma < 0$, the critical point $(0, m)$ is a saddle point. When $\sigma > 0$, the critical point $(0, m)$ is an unstable nodal source.

Next we shall show there is a heteroclinic orbit connecting the critical points (u_+, v_+) and (u_-, v_-).

Case i: $\sigma < 0$

When $\sigma < 0$, similar to above analysis, we can prove the region $\mathcal{G}$ (see Figure 3.2) enclosed by these two curves is an invariant region of system (3.9). The region $\mathcal{G} = \{(U, V) \mid 0 \leq U \leq -\sigma V^2 - cV + \rho_2, \ V \geq -c\}$ is bounded by

$$\Gamma_1 = \{(U, V) \mid V = -c, \ 0 < U < u_-\},$$
$$\Gamma_2 = \{(U, V) \mid U = -\sigma V^2 - cV + \rho_2, \ 0 < U < u_-, \ -c < V < v_+\},$$
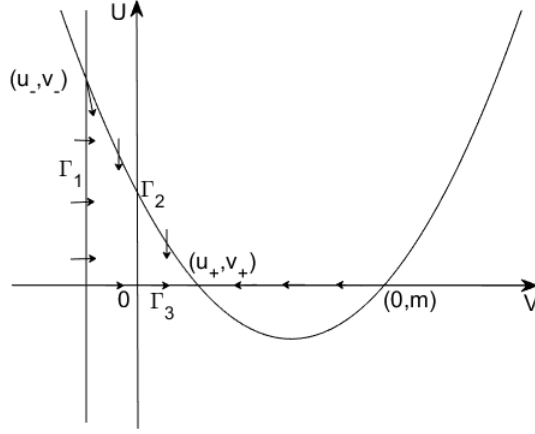$$\Gamma_3 = \{(U, V) \mid U = 0, \ -c < V < v_+\}.$$

Figure 3.2: Phase portrait for $\rho_1 = 0$ and $\sigma < 0$

To this end, we shall show that the unstable manifold of system (3.9) emanating from the saddle point (u_-, v_-) points inside the invariant region $\mathcal{G}$. From direct calculation, we derive the tangent direction of Γ_1 at (u_-, v_-) is $\frac{dU}{dV}\big|^{\Gamma_1}_{(u_-, v_-)} = -\infty$ and the tangent direction of Γ_2 at (u_-, v_-) is $\frac{dU}{dV}\big|^{\Gamma_2}_{(u_-, v_-)} = (2\sigma - 1)c$.

Next we derive the direction of the unstable manifold of system (3.9) at the saddle point (u_-, v_-) and make comparisons with the directions of nullclines calculated above. We consider the positive eigenvalue of $\hat{J}(u_-, v_-)$ is $\gamma_2 = \frac{(2\sigma-1)c}{2\varepsilon} + \frac{1}{2}\sqrt{\frac{(2\sigma-1)^2 c^2}{\varepsilon^2} + \frac{4u_-}{\varepsilon d}}$ which has the eigenvector $R_2 = \begin{bmatrix} -\frac{u_-}{d} \\ \gamma_2 \end{bmatrix}$. Hence the slope of the unstable manifold of (3.9) at (u_-, v_-) is

$$\frac{dU}{dV}\bigg|_{(u_-, v_-)} = (2\sigma - 1)c - \varepsilon\gamma_2$$

One can easily check that

$$-\infty = \frac{dU}{dV}\bigg|^{\Gamma_1}_{(u_-, v_-)} < \frac{dU}{dV}\bigg|_{(u_-, v_-)} < \frac{dU}{dV}\bigg|^{\Gamma_2}_{(u_-, v_-)} = (2\sigma - 1)c$$

On the other hand, at the saddle point $(0, m)$, the eigenvector of the positive eigen-

25

value γ_2 is $R_2 = \begin{bmatrix} 0 \\ \alpha \end{bmatrix}$ which is along the V-axis and hence can not form a non-trivial

trajectory. Therefore we deduce that the direction of the unstable manifold of (3.9) at (u_-, v_-) is between the tangent lines of Γ_2 and Γ_1 at (u_-, v_-) which points inside the region $\mathcal{G}$. On the basis of the Poincaré-Bendixson theorem, this unstable manifold has to reach the stable equilibrium (u_+, v_+). This trajectory connecting (u_-, v_-) and (u_+, v_+) generates a solution for the system (3.9) with $U_z < 0$ and $V_z > 0$.

Case ii: $\sigma > 0$

When $\sigma > 0$, similar to above analysis, we can prove the region $\mathcal{G}$ bounded by Γ_1, Γ_2 and Γ_3 (see Figure 3.3) enclosed by these two curves is an invariant region of system (3.9).

(a) Phase portrait for $0 < \sigma \leq \frac{1}{2}$ (b) Phase portrait for $\sigma > \frac{1}{2}$
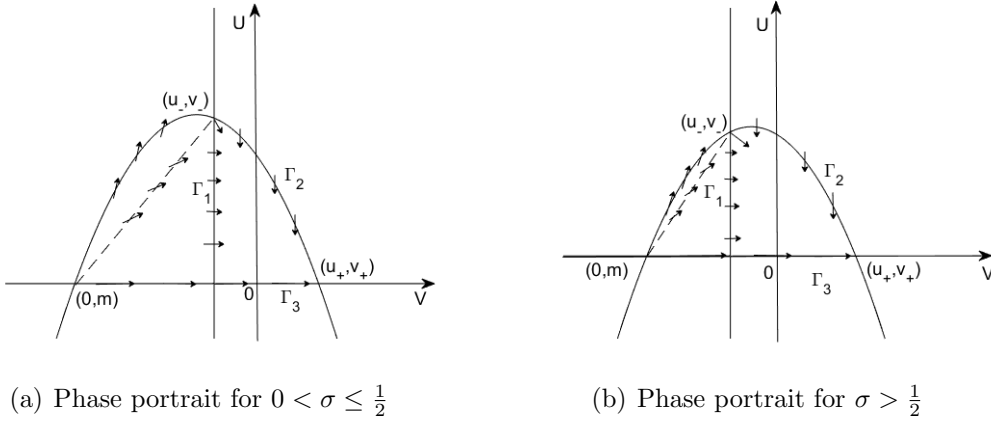
Figure 3.3: Phase portraits for $\rho_1 = 0$ and $\sigma > 0$

Also, one can easily check

$$-\infty = \frac{dU}{dV}\bigg|_{(u_-,v_-)}^{\Gamma_1} < \frac{dU}{dV}\bigg|_{(u_-,v_-)} < \frac{dU}{dV}\bigg|_{(u_-,v_-)}^{\Gamma_2} = (2\sigma - 1)c$$

This shows that the unstable manifold of the saddle point (u_-, v_-) points inside $\mathcal{G}$. Since there is no other critical points inside $\mathcal{G}$, by the Poincaré-Bendixson theorem the unstable manifold emanating from the saddle point (u_-, v_-) to reach the stable

26

nodal sink (u_+, v_+) eventually. Such a trajectory generates a traveling wave solution for the system with $U_z < 0$, $V_z > 0$.

Then we need to calculate $\frac{dU}{dV}|_{(0,m)}$ to rule out the possibility that the unstable node $(0, m)$ connects to the critical points (u_+, v_+) and (u_-, v_-). The Jacobian matrix at $(0, m)$ is

$$\hat{J}(0, m) = \begin{bmatrix} -\frac{c+m}{d} & 0 \\ -\frac{1}{\varepsilon} & -\frac{c+2\sigma m}{\varepsilon} \end{bmatrix}$$

which has two positive eigenvalues $\gamma_1 = -\frac{c+m}{d} > 0$, $\gamma_2 = -\frac{c+2\sigma m}{\varepsilon} > 0$. The corresponding eigenvector of γ_1 is $R_1 = \begin{bmatrix} -\varepsilon\beta(-\frac{c+m}{d} + \frac{c+2\sigma m}{\varepsilon}) \\ \beta \end{bmatrix}$. The corresponding eigenvector of γ_2 is $R_2 = \begin{bmatrix} 0 \\ \alpha \end{bmatrix}$ which is along the V-axis and hence can not form a non-trivial trajectory. Now we turn to consider the direction of the unstable manifold at the unstable node $(0, m)$, which is

$$\frac{dU}{dV}\Big|_{(0,m)} = -\varepsilon(-\frac{c+m}{d} + \frac{c+2\sigma m}{\varepsilon})$$

$$= \frac{\varepsilon}{d}(c + m) - (c + 2\sigma m)$$

$$< -(c + 2\sigma m)$$

The slope of the tangent line of the parabola $U = -\sigma V^2 - cV + \rho_2$ at $(0, m)$ is

$$\frac{dU}{dV}\Big|_{(0,m)} = -2\sigma m - c = -(c + 2\sigma m) > 0$$

Hence the unstable manifold of the eigenvalues γ_1 can not enter the invariant region $\mathcal{G}$. Outside the region enclosed by the parabola and V-axis, we know that $V_z < 0$, hence the trajectories always point to the left.

Therefore, from above analysis, when $\rho_1 = 0$, there only exist trajectories connecting

27

(u_+, v_+) and (u_-, v_-) which correspond to a traveling wave solution of the system with $U_z < 0$, $V_z > 0$. Combining (3.19) (3.20) (3.13), the proof of first part of Theorem 3.1 is completed.

3.2.2   Case of $\rho_1 \neq 0$

From (3.4), we see that

$$
\begin{aligned}
\mathcal{H}(\lambda_2(u_-, v_-), u_-, v_-) =& \frac{1}{d\varepsilon}\Bigg(\Big(-\frac{(2\sigma+1)v_-}{2} + \frac{\sqrt{(2\sigma-1)^2 v_-^2 + 4u_-}}{2}\Big)^2 \\
&+ (2\sigma+1)v_-\Big(-\frac{2\sigma+1)v_-}{2} + \frac{\sqrt{(2\sigma-1)^2 v_-^2 + 4u_-}}{2}\Big) + 2\sigma v_-^2 - u_-\Bigg) \\
=& \frac{1}{d\varepsilon}\Big(-\frac{(2\sigma+1)v_-^2}{4} + \frac{(2\sigma-1)^2 v_-^2}{4} + u_- + 2\sigma v_- u_-\Big) \\
=& \frac{1}{d\varepsilon}\Big(\frac{\big((2\sigma-1)^2 - (2\sigma+1)^2\big)v_-^2}{4} + 2\sigma v_-^2\Big) \\
=& 0
\end{aligned}
$$

Also, $\mathcal{H}(\lambda_2(u_+, v_+), u_+, v_+) = \mathcal{H}(\lambda_2(u_-, v_-), u_-, v_-) = 0$.

Using the entropy condition (3.16) and from the definition of $\lambda_1(u, v)$ in (3.4), we know that $\lambda_1(u_-, v_-) < c$ and we can show that

$$\gamma_1 \gamma_2|_{(u_-, v_-)} = \mathcal{H}(c, u_-, v_-) < \mathcal{H}(\lambda_2(u_-, v_-), u_-, v_-) = 0$$

$$\gamma_1 \gamma_2|_{(u_+, v_+)} = \mathcal{H}(c, u_+, v_+) > \mathcal{H}(\lambda_2(u_+, v_+), u_+, v_+) = 0$$

We know $c + v_+ > c + v_- \geq 0$ from (3.15), then

$$\gamma_1 + \gamma_2|_{(u_\pm, v_\pm)} = -\Big(\frac{c + v_\pm}{d} + \frac{c + 2\sigma v_\pm}{\varepsilon}\Big) < 0$$

28

Therefore the equilibrium (u_+, v_+) is a stable node and (u_-, v_-) is a saddle point.

Next we look at the nullclines of system (3.7) which are given by

$$\begin{cases} U(V + c) = \rho_1, \\ U = -\sigma V^2 - cV + \rho_2. \end{cases} \tag{3.21}$$

We shall show that the region $\mathcal{G}$ enclosed by these two curves composes an invariant region of system (3.9) (3.8), which is defined by

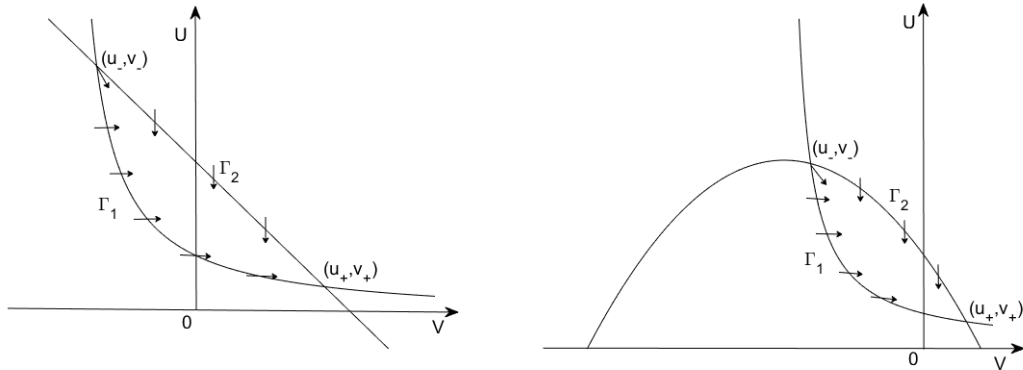$$\mathcal{G} = \left\{ (U, V) \mid \frac{\rho_1}{V + c} \leq U \leq \sigma V^2 - cV + \rho_2 \right\} \tag{3.22}$$

The edges of the region $\mathcal{G}$ are denoted by

$$\Gamma_1 = \{(U, V) \mid U = \frac{\rho_1}{V + c}, \ u_+ < U < u_-, \ v_- < V < v_+\},$$

$$\Gamma_2 = \{(U, V) \mid U = -\sigma V^2 - cV + \rho_2, \ u_+ < U < u_-, \ v_- < V < v_+\}.$$

Case 1: $\sigma \geq 0$

When $\sigma \geq 0$, there are only two equilibria (u_+, v_+) and (u_-, v_-).

(a) Phase portrait for $\sigma = 0$ (b) Phase portrait for $\sigma > 0$

Figure 3.4: Phase portrait for $\rho_1 \neq 0$ and $\sigma \geq 0$

When $\sigma = 0$, the first equation of (3.21) gives a hyperbola and the second equation of (3.21) gives a straight line (see Figure 3.4(a)). When $\sigma > 0$, the second

equation gives a parabola (see Figure 3.4(b)). From the same analysis, along the edge $\Gamma_1 : U_z = 0$ and $V_z|_{(U,V)\in\Gamma_1} > 0$ which means the direction field of (3.9) a-long the edge Γ_1 points to the right horizontally. Along the edge $\Gamma_2 : V_z = 0$ and $U_z|_{(U,V)\in\Gamma_2} < 0$ which means the direction field of (3.9) along the edge Γ_2 points downwards. Therefore $\mathcal{G}$ is an invariant region of system (3.9). The phase portrait is illustrated in Figure 3.4.

To prove that the heteroclinic connection between (u_-, v_-) and (u_+, v_+), we shall show that the unstable manifold of system (3.9) emanating from the saddle point (u_-, v_-) points inside the invariant region $\mathcal{G}$.

To this end, we calculate the tangent directions of the nullclines at (u_-, v_-). Solving V from the first equation of (3.21) and differentiating with respect to U, we derive

$$\frac{dU}{dV}\Big|_{(u_-,v_-)}^{\Gamma_1} = -\frac{\rho_1}{(V+c)^2}\Big|_{(u_-,v_-)} = -\frac{u_-}{c+v_-} \tag{3.23}$$

where $\frac{dU}{dV}\Big|_{(u_-,v_-)}^{\Gamma_1}$ denotes the tangent direction of Γ_1 at (u_-, v_-). From the second equation of (3.21), we derive

$$\frac{dU}{dV}\Big|_{(u_-,v_-)}^{\Gamma_2} = -(c + 2\sigma v_-) < 0 \tag{3.24}$$

where $\frac{dU}{dV}\Big|_{(u_-,v_-)}^{\Gamma_2}$ denotes the tangent direction of Γ_2 at (u_-, v_-).

Next we derive the direction of the unstable manifold of system (3.9) at the saddle (u_-, v_-) and make comparisons with the directions of the nullclines calculated above. To this end, we consider the positive eigenvalue of $\hat{J}(u_-, v_-)$,

$$\gamma_2 = -\frac{\frac{c+v_-}{d} + \frac{c+2\sigma v_-}{\varepsilon}}{2} + \frac{\sqrt{(\frac{c+v_-}{d} - \frac{c+2\sigma v_-}{\varepsilon})^2 + \frac{4u_-}{\varepsilon d}}}{2}$$

which has the following eigenvector

30

$$R_2 = \begin{bmatrix} -\frac{u_-}{d} \\ \gamma_2 + \frac{c+v_-}{d} \end{bmatrix}$$

Tangent to the eigenvector R_2, the direction of the unstable manifold of (3.9) at (u_-, v_-) is given by

$$\begin{aligned}
\frac{dU}{dV}\Big|_{(u_-,v_-)} &= \frac{-\frac{u_-}{d}}{\gamma_2 + \frac{c+v_-}{d}} \\
&= \frac{-\varepsilon(\gamma_2 + \frac{c+v_-}{d})(\gamma_2 + \frac{c+2\sigma v_-}{\varepsilon})}{\gamma_2 + \frac{c+v_-}{d}} \\
&= -\varepsilon\gamma_2 - (c + 2\sigma v_-) \\
&< -(c + 2\sigma v_-)
\end{aligned} \tag{3.25}$$

On the other hand, since $\gamma_2 > 0$, we have

$$\frac{-\frac{u_-}{d}}{\gamma_2 + \frac{c+v_-}{d}} > \frac{-\frac{u_-}{d}}{\frac{c+v_-}{d}} = -\frac{u_-}{c+v_-}. \tag{3.26}$$

Therefore, combining (3.23), (3.24), (3.25), we end up with

$$\frac{dV}{dU}\Big|_{(u_-,v_-)}^{\Gamma_1} < \frac{dV}{dU}\Big|_{(u_-,v_-)} < \frac{dV}{dU}\Big|_{(u_-,v_-)}^{\Gamma_2} \tag{3.27}$$

where the left hand side of (3.27) represents the tangential direction of the edge Γ_2 at (u_-, v_-), the right-hand side of (3.27) is the tangential direction of the edge Γ_1 at (u_-, v_-), and the middle term of (3.27) is the direction of unstable manifold of system (3.9) at (u_-, v_-). Therefore we deduce that the direction of the unstable manifold of (3.9) at (u_-, v_-) is between the tangent lines of Γ_2 and Γ_1 at (u_-, v_-) which points inside the region $\mathcal{G}$. On the basis of the Poincaré-Bendixson theorem, this unstable manifold has to reach the stable equilibrium (u_+, v_+). This trajectory connecting (u_-, v_-) and (u_+, v_+) generates a solution for the system (3.9) with

31

$U_z < 0$ and $V_z > 0$.

Case 2: $\sigma < 0$

When $\sigma < 0$, there are three critical points (u_+, v_+), (u_-, v_-) and $(p, q) = (-\frac{\sigma \rho_1}{c + \sigma v_+ + \sigma v_-}, -\frac{c(\sigma+1)}{\sigma} - v_+ - v_-)$. Using the entropy condition (3.16) and $\lambda_1(u_*, v_*) < 0 < c$, we can know that (u_+, v_+) is a stable node and (u_-, v_-) is a saddle point. Then we have three different cases as sketched below.
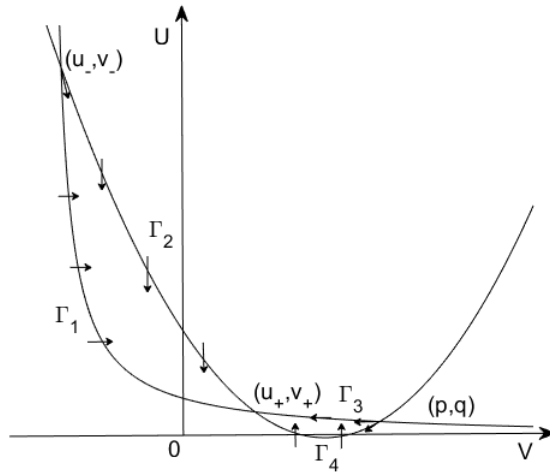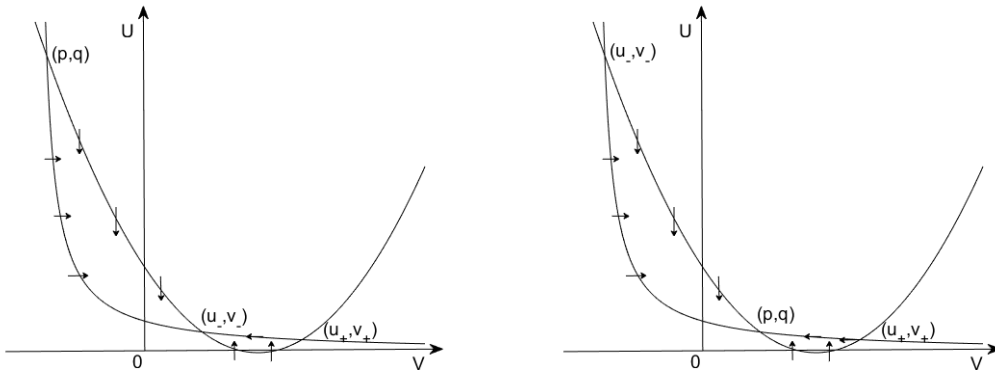

Figure 3.5: Phase portrait for $\rho_1 \neq 0$, $\sigma < 0$ and $q > v_+ > v_-$

(a) Phase portrait for $\sigma < 0$ and $v_+ > v_- > q$ (b) Phase portrait for $\sigma < 0$ and $v_+ > q > v_-$

Figure 3.6: Phase portrait for $\rho_1 \neq 0$, $\sigma < 0$

32

However, in Figure 3.6, (u_+, v_+) is on the right hand side of the symmetry axis $V = -\frac{c}{2\sigma}$ which means $v_+ > 0$ and $-2\sigma v_+ > c$. Then according to the definition of $\lambda_2(u, v)$ in (3.4), we have $\lambda_2(u_+, v_+) > -2\sigma v_+ > c$ which doesn't satisfy the entropy condition $\lambda_2(u_+, v_+) < c$ in (3.16). Hence we only consider the case $q > v_+ > v_-$ and the phase portrait is illustrated in Figure 3.5. Also, we know (p, q) is on the right hand side of the symmetry axis of the parabola $V = -\frac{c}{2\sigma}$ from which we can have

$$\sigma(v_+ + v_-) + (\frac{1}{2} + \sigma)c > 0 \tag{3.28}$$

Using the same phase plane analysis as that of the case $\rho_1 \neq 0$ and $\sigma \geq 0$, we can conclude there exists a traveling wave emanating from the saddle point (u_-, v_-) to reach the stable node (u_+, v_+) eventually with $U_z < 0$ and $V_z > 0$.

Next we consider that the invariant region $\mathcal{S}$ which is defined by

$$\mathcal{S} = \left\{ (U, V) \mid -\sigma V^2 - cV + \rho_2 \leq U \leq \frac{\rho_1}{V + c} \right\}$$

The edges of the region $\mathcal{S}$ are denoted by

$$\Gamma_3 = \{(U, V) \mid U = \frac{\rho_1}{V + c}, \ p < U < u_+, \ v_+ < V < q\},$$

$$\Gamma_4 = \{(U, V) \mid U = -\sigma V^2 - cV + \rho_2, \ p < U < u_+, \ v_+ < V < q\}.$$

We have already knew $\lambda_1(p, q) < 0 < c$. The point (p, q) is on the right hand side of the symmetry axis of the parabola $V = -\frac{c}{2\sigma}$ which means $q > 0$ and $-2\sigma q > c$. Then according to the definition of $\lambda_2(u, v)$ in (3.4), we have $\lambda_2(p, q) > -2\sigma q > c$. Therefore $\gamma_1 \gamma_2|_{(p,q)} < 0$ and the critical point (p, q) is a saddle point. The tangent direction of the parabola at the saddle point (p, q) is $\frac{dU}{dV}|_{(p,q)}^{\Gamma_4} = -(c + 2\sigma q) > 0$. The tangent direction of the hyperbola at the saddle point (p, q) is $\frac{dU}{dV}|_{(p,q)}^{\Gamma_3} = -\frac{p}{c+q} < 0$. To this end, we consider the positive eigenvalue of $\hat{J}(p, q)$,

$$\gamma_2 = -\frac{\frac{c+q}{d} + \frac{c+2\sigma q}{\varepsilon}}{2} + \frac{\sqrt{(\frac{c+q}{d} - \frac{c+2\sigma q}{\varepsilon})^2 + \frac{4p}{\varepsilon d}}}{2}$$

33

which has the following eigenvector

$$R_2 = \begin{bmatrix} -\frac{p}{d} \\ \gamma_2 + \frac{c+q}{d} \end{bmatrix}$$

Then from direct calculation, we can have

$$
\begin{aligned}
\frac{dU}{dV}\Big|_{(p,q)} &= \frac{-\frac{p}{d}}{\gamma_2 + \frac{c+q}{d}} \\
&= \frac{-\varepsilon\left(\gamma_2 + \frac{c+q}{d}\right)\left(\gamma_2 + \frac{c+2\sigma q}{\varepsilon}\right)}{\gamma_2 + \frac{c+q}{d}} \\
&= -(c + 2\sigma q) - \varepsilon\gamma_2 \\
&= \frac{\varepsilon}{2}\left(\frac{c+q}{d} - \frac{c+2\sigma q}{\varepsilon} - \sqrt{(\frac{c+q}{d} - \frac{c+2\sigma q}{\varepsilon})^2 + \frac{4p}{\varepsilon d}}\right) \\
&< 0
\end{aligned}
$$

Hence, we end up with

$$\frac{dU}{dV}\Big|_{(p,q)}^{\Gamma_3} < \frac{dU}{dV}\Big|_{(p,q)} < 0 < \frac{dU}{dV}\Big|_{(p,q)}^{\Gamma_4}$$

Therefore, such a trajectory corresponds to a traveling wave solution of the system with $U_z > 0$ and $V_z < 0$ which means the unstable manifold emanating from the saddle point (p,q) goes to the stable nodal sink (u_+, v_+) eventually. However, it doesn't satisfy the entropy condition (3.16) which makes the results have more realistic physical meaning. Therefore there exists a monotone traveling wave which satisfies $U_z < 0$ and $V_z > 0$. Then the proof of second part of Theorem 3.1 is completed.

Chapter 4

Numerical Simulations of wave propogation

In this chapter, we present corresponding numerical simulations of wave propagation for cases $\rho_1 = 0$ and $\rho_1 \neq 0$ and we shall focus on the applications of system (1.4) in biological systems. Here we use method of line to simulated the wave propagation in a finite spatial domain, $\Omega = (0, 350)$, with no-flux boundary condition and the initial data are taken to be

$$u_0(x) = \bar{u} + \frac{1}{1 + e^{(2(x-50))}},$$

$$v_0(x) = \bar{v} + \frac{1}{1 + e^{(-2(x-50))}}.$$

(4.1)

which is motivated by [21].

First, we simulate the traveling wave phenomena with $\sigma = 0$ in Figure 4.1 and Figure 4.2. It is a special case of the attraction-repulsion chemotaxis model which describes the aggregation of *Microglia* in Alzhemer's disease. In Figure 4.1, we choose parameter values as $d = 0.5$, $\varepsilon = 15$, $\chi = 1$ and $\sigma = 0$ to be compatible with the data in [22] where the authors emphasize the motility of chemical signals is much larger than the diffusion rate of cells (i.e. $d \ll \varepsilon$).
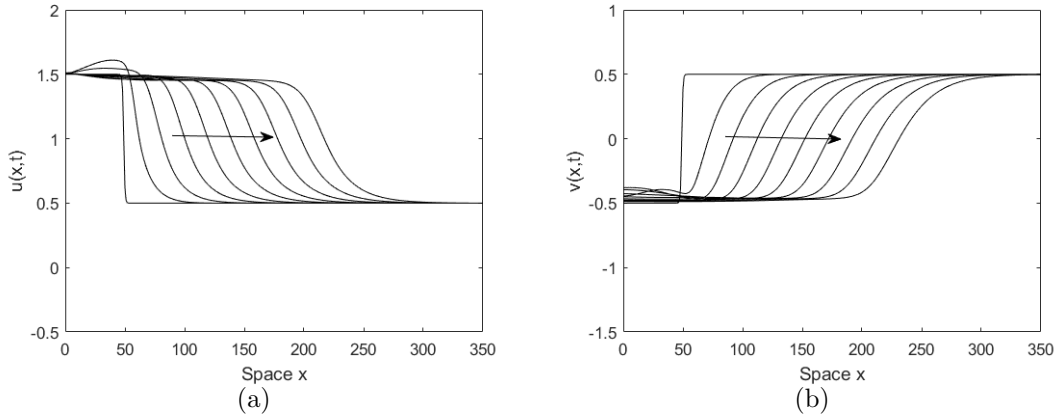
(a)　　　　　　　　　　　　　(b)

Figure 4.1: Numerical simulation of traveling wavefront u of model (1.4) with $d = 0.5$, $\varepsilon = 15$, $\chi = 1$, $\sigma = 0$, $\rho_1 \neq 0$ and initial data are $\bar{u} = 0.5$, $\bar{v} = -0.5$. The arrow indicated the propagating direction of traveling waves.
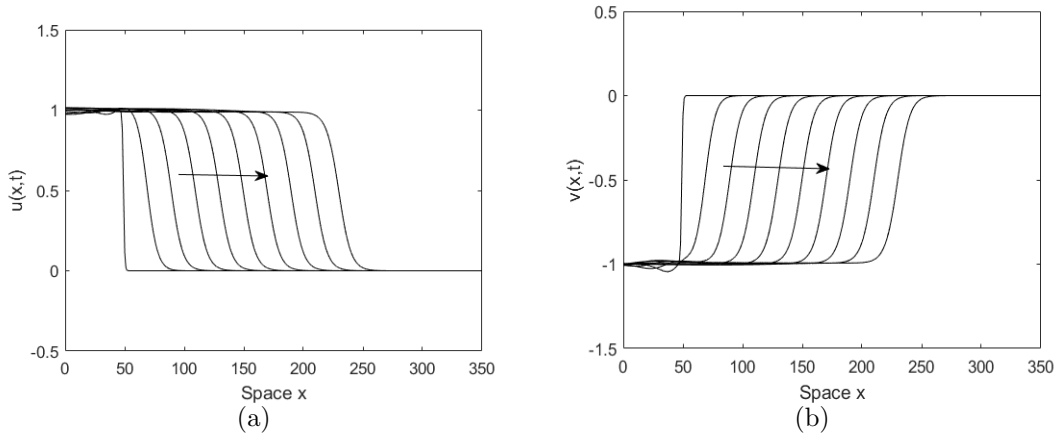

(a)　　　　　　　　　　　　　(b)

Figure 4.2: Numerical simulation of traveling wavefront u of model (1.4) with $d = 5$, $\varepsilon = 0.3$, $\chi = 1$, $\sigma = 0$, $\rho_1 = 0$ and initial data are $\bar{u} = 0$, $\bar{v} = -1$. The arrow indicated the propagating direction of traveling waves.

By contrast, in the following two cases, the diffusion rate of chemicals is much smaller than the diffusion rate of cells. In Figure 4.3 and Figure 4.4, we study the wave propagation of model (1.4) with $d = 5$, $\chi = 1$ and $\varepsilon = 0.3$. When $\sigma = -\varepsilon$, it's a system transformed from a chemotaxis system about the initiation angiogenesis. Moreover, patterns of traveling are also numerically presented in [21, 41] which de-

36

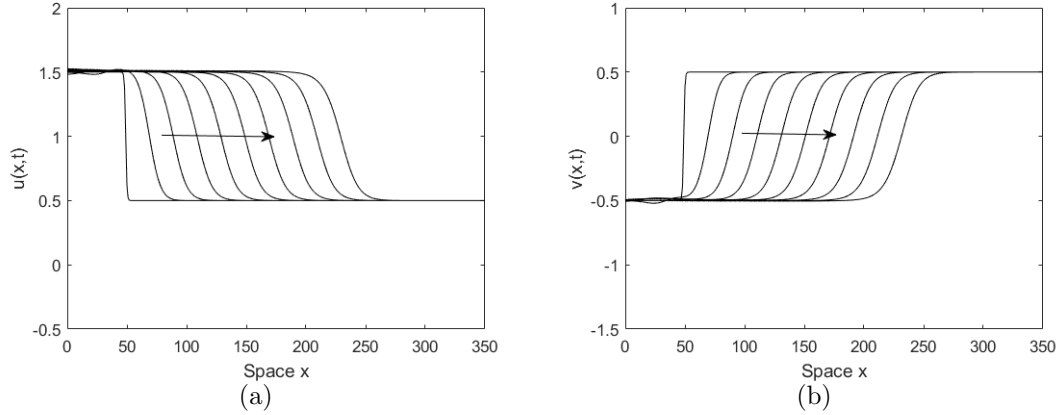scribes the directed migration of endothecial cells towards the signalling molecules VEGF.

(a)   (b)

Figure 4.3: Numerical simulation of traveling wavefront u of model (1.4) with $d = 5$, $\varepsilon = 0.3$, $\chi = 1$, $\sigma = -0.3$, $\rho_1 \neq 0$ and initial data are $\bar{u} = 0.5$, $\bar{v} = -0.5$. The arrow indicated the propagating direction of traveling waves.
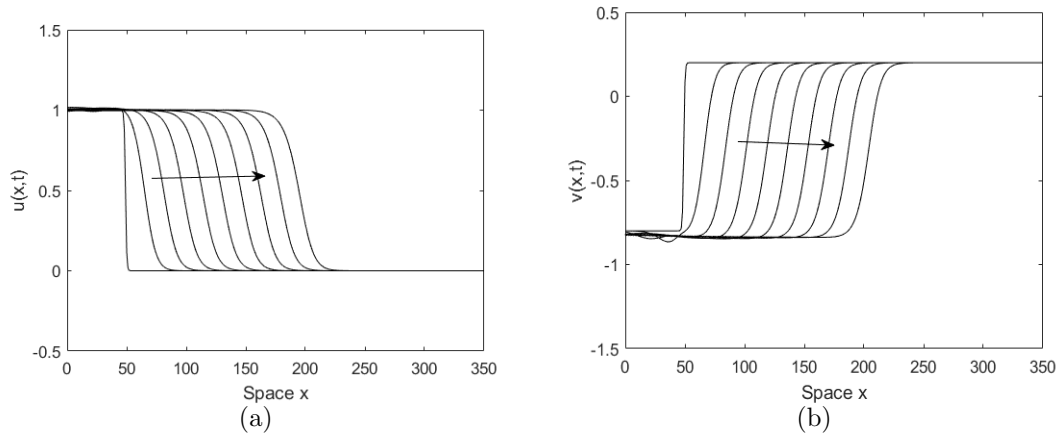

(a)   (b)

Figure 4.4: Numerical simulation of traveling wavefront u of model (1.4) with $d = 5$, $\varepsilon = 0.3$, $\chi = 1$, $\sigma = -0.1$, $\rho_1 = 0$ and initial data are $\bar{u} = 0$, $\bar{v} = -0.8$. The arrow indicated the propagating direction of traveling waves.

Figure 4.5 and Figure 4.6 perform propagating waves generated by the model (1.4) transformed from the system (1.7) with $d = 5$, $\chi = 1$, $\varepsilon = 0.3$ and $\sigma = \varepsilon = 0.3$.

37

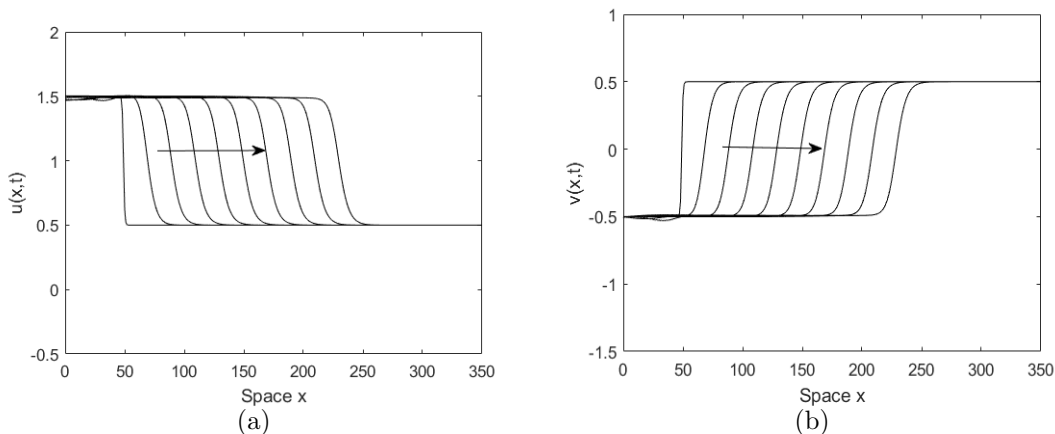The model (1.7) accounts for the chemotactic movement of reinforced random walker.

Figure 4.5: Numerical simulation of traveling wavefront u of model (1.4) with $d = 5$, $\varepsilon = 0.3$, $\chi = 1$, $\sigma = 0.3$, $\rho_1 \neq 0$ and initial data are $\bar{u} = 0.5$, $\bar{v} = -0.5$. The arrow indicated the propagating direction of traveling waves.
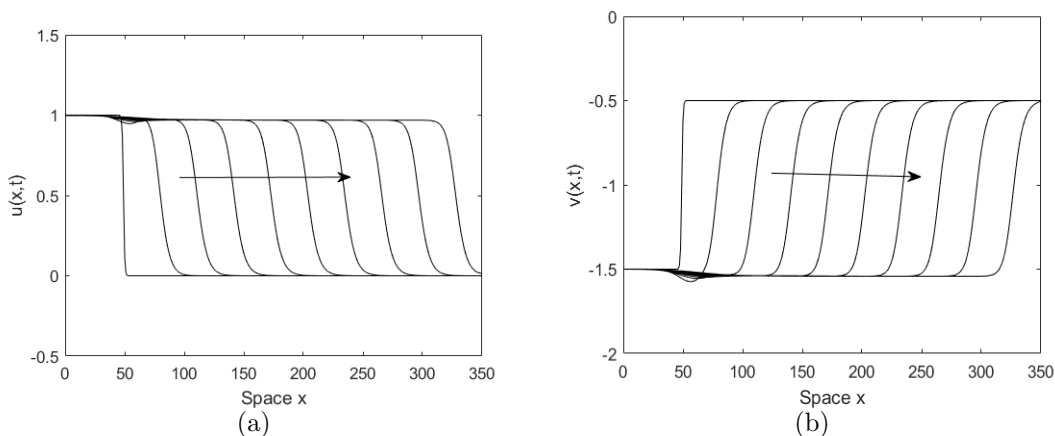

Figure 4.6: Numerical simulation of traveling wavefront u of model (1.4) with $d = 5$, $\varepsilon = 0.3$, $\chi = 1$, $\sigma = 0.3$, $\rho_1 = 0$ and initial data are $\bar{u} = 0$, $\bar{v} = -1.5$. The arrow indicated the propagating direction of traveling waves.

Finally, we show some numerical results with $|\sigma|$ large to see the behavior of traveling wave of u. We consider three sets of parameter values: (1) $\sigma = -2$ with initial

38

data, $\bar{u} = 0.5$ and $\bar{v} = -0.5$; (2) $\sigma = -2$ with initial data, $\bar{u} = 0$ and $\bar{v} = -1$; (3) $\sigma = 1.5$ with initial data, $\bar{u} = 0$ and $\bar{v} = -1$. Then from Figure 4.7, Figure 4.8 and Figure 4.9, as the propagating of wave, we can see there are some small oscillations showing on the traveling wave. Moreover, when $\sigma < 0$, the oscillations occurs on the head of the wave (See Figure 4.7 and Figure 4.8). When $\sigma > 0$, the oscillations propagates from the tail of the wave to the head of the wave (See Figure 4.9).
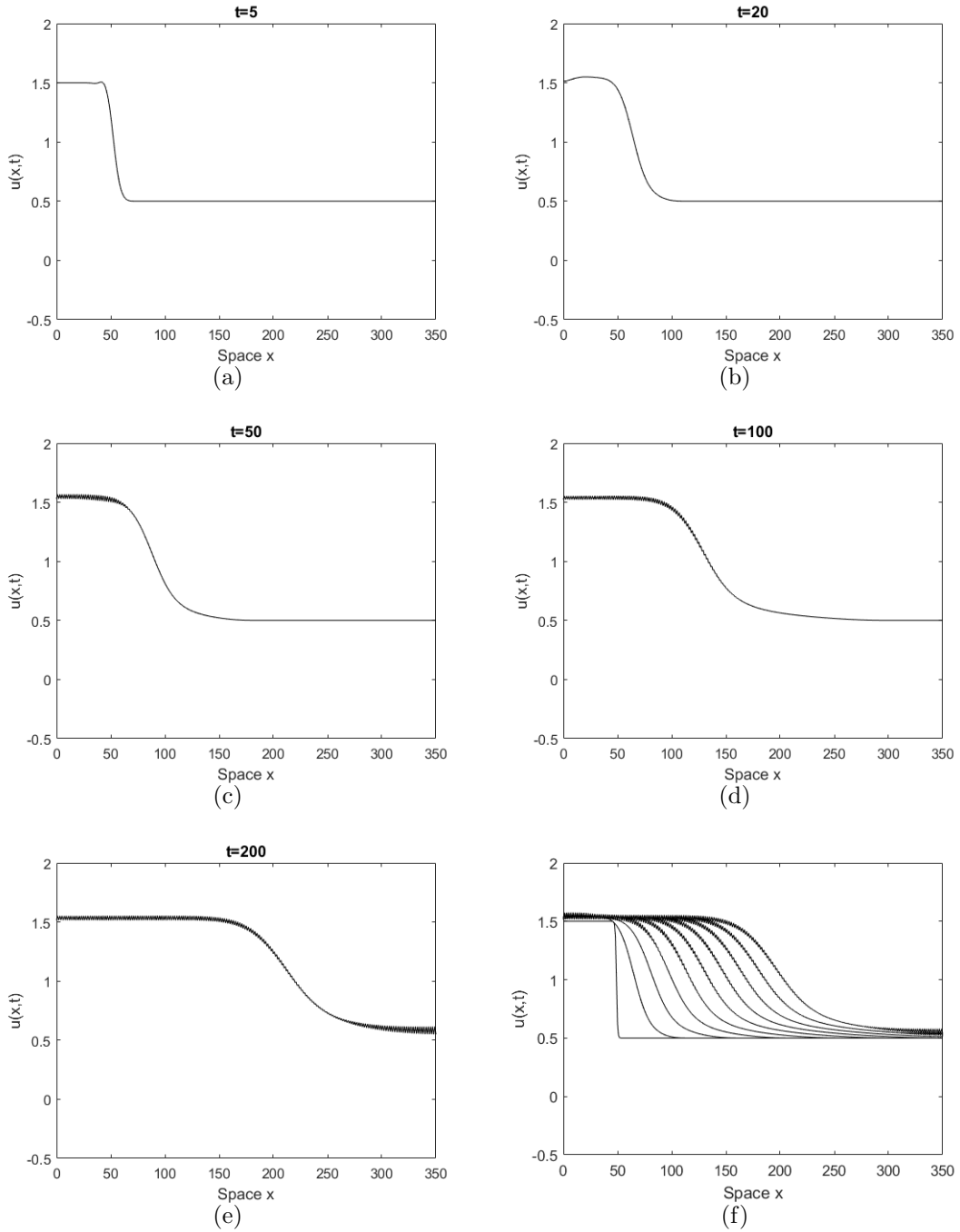
Figure 4.7: Numerical simulation of traveling wavefront u of model (1.4) with $d = 5$, $\varepsilon = 0.3$, $\chi = 1$, $\sigma = -2$ and initial data are $\bar{u} = 0.5$, $\bar{v} = -0.5$.

Figure 4.8: Numerical simulation of traveling wavefront u of model (1.4) with $d = 5$, $\varepsilon = 0.3$, $\chi = 1$, $\sigma = -2$ and initial data are $\bar{u} = 0$, $\bar{v} = -1$.

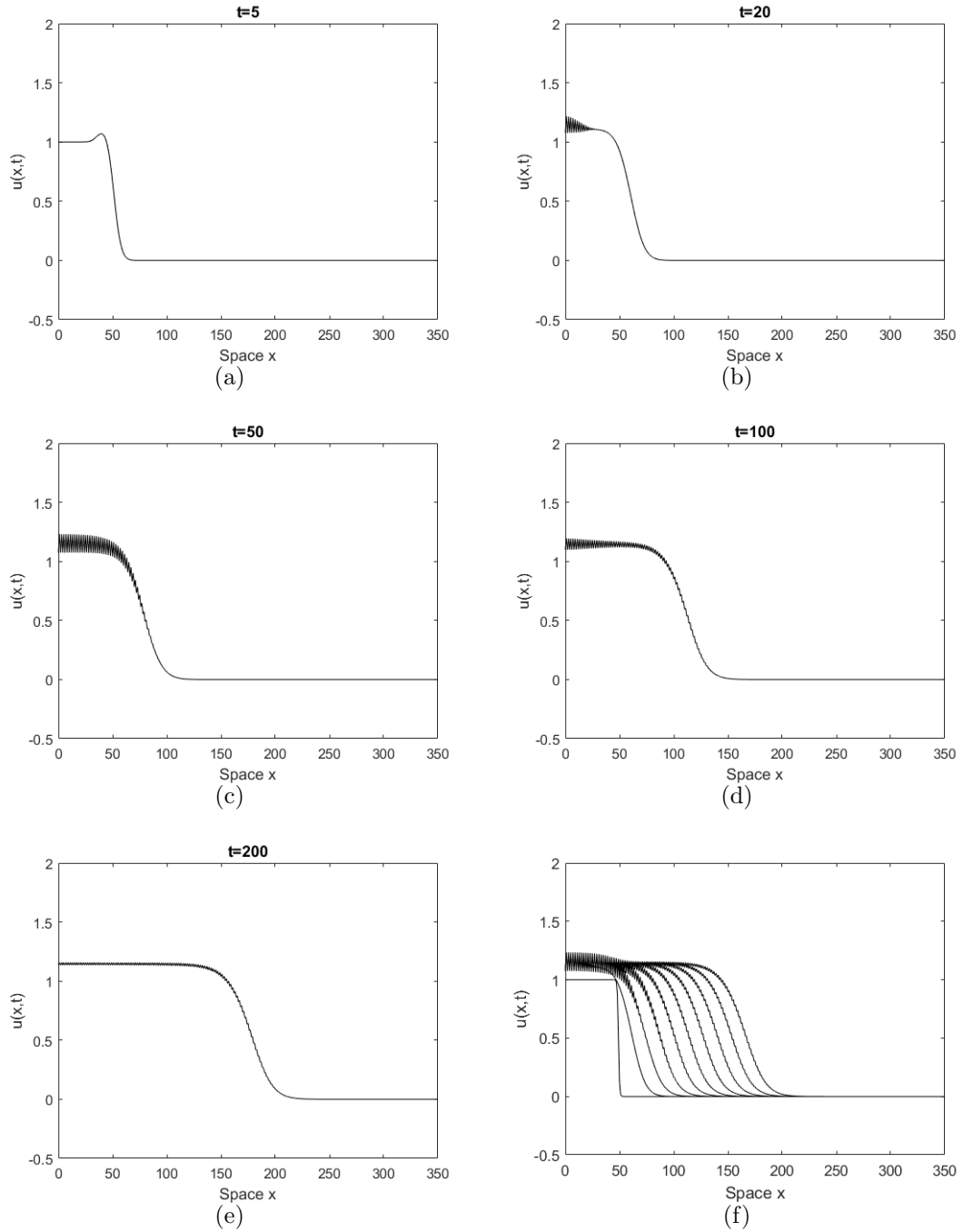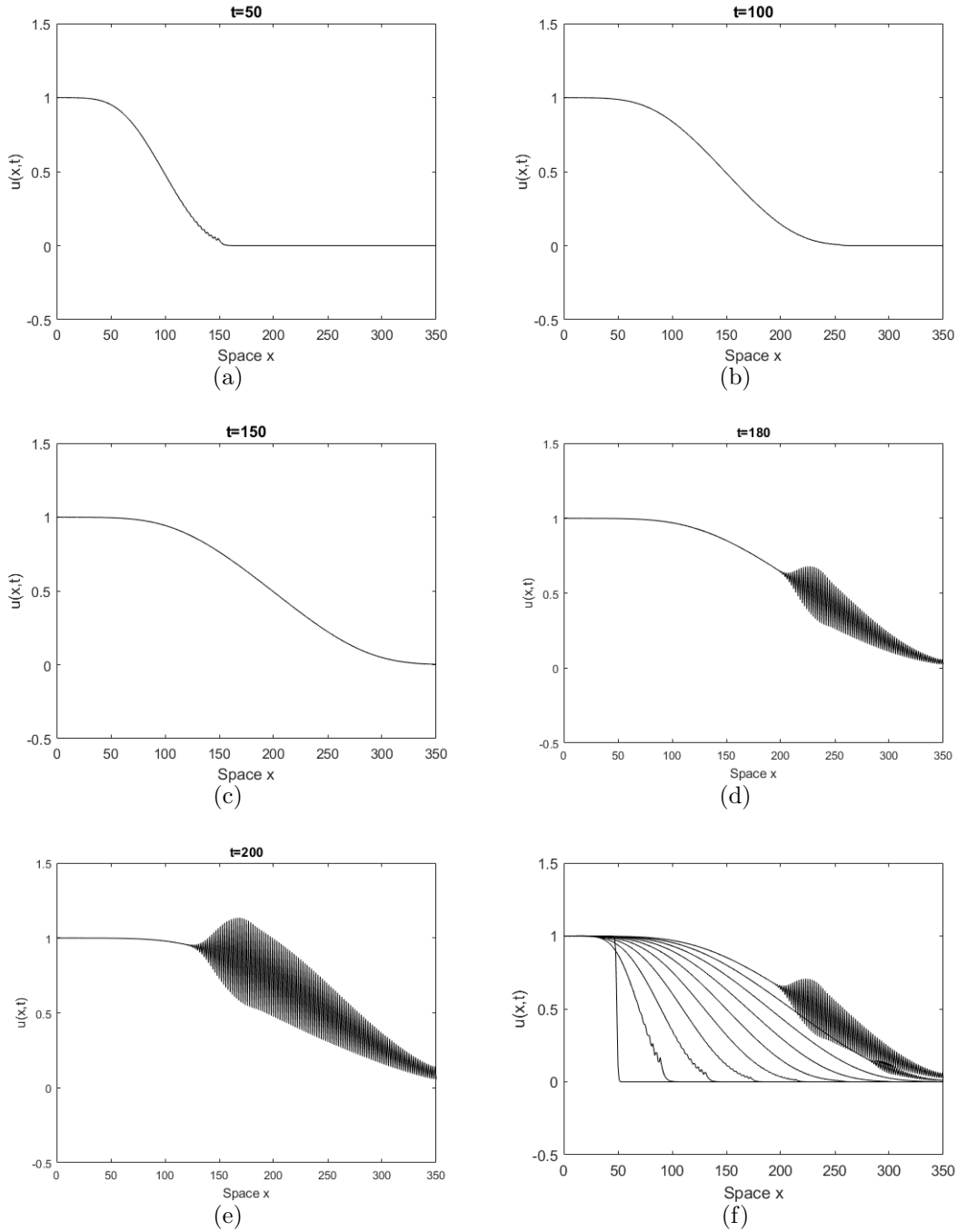Figure 4.9: Numerical simulation of traveling wavefront u of model (1.4) with $d = 5$, $\varepsilon = 0.3$, $\chi = 1$, $\sigma = 1.5$ and initial data are $\bar{u} = 0$, $\bar{v} = -1$.

Chapter 5

Conclusions and Future work

This thesis established the existence of traveling wave solutions for system (1.4) which has very prominent applications in biomedical or biological sciences. Then we proved the existence of traveling wave solutions by the phase plane analysis. Despite abundant results obtained in [9, 10, 41], there are still many interesting questions remain to be solved.

The first point is about the smallness assumption for $|\sigma|$. From Figure 4.7, Figure 4.8 and Figure 4.9 in Chapter 4, it's easy to see the solution behavior showed by numerical results for large $|\sigma|$ with $u_+ \geq 0$ is different from the situation for small $|\sigma|$. When $|\sigma|$ is large, the system (1.4) is no longer hyperbolic. Hence the existence of traveling wave solutions for large $|\sigma|$ needs to be examined by different methods. On the other hand, the stability / instability of traveling wave solutions is another interesting problem. The stability result for Keller-Segel [12] was obtained in [26]. Nonlinear stability of the model (1.4) with $\sigma = -\varepsilon$ was proved in [20] by method of energy estimates and then the results of transformed model were transferredback to the original Keller-Segel chemotaxis model in [21]. Although there are many gorgeous results obtained in previous studies [41], it remains open to study the property of the system in general form (1.4). In addition, the assumption of small initial perturbations is needed in [19, 20, 41] to study the stability. However, the

numerical simulations in [41] shows the stability of traveling waves with large initial perturbations which is deserved to be examined in the future.

Moreover, the study of existence of two dimensional traveling wave solutions (e.g., planar waves) is also another important problem that is worthwhile to be explored in the future.

Bibliography

[1] J. Adler. Chemotaxis in bacteria. *Science*, 153(3737):708–716, 1966.

[2] J. Adler. Chemotaxis in bacteria. *Annual review of biochemistry*, 44(1):341–356, 1975.

[3] S. Childress. Chemotactic collapse in two dimensions. In *Modelling of patterns in space and time*, pages 61–66. Springer, 1984.

[4] I. Cohen, I. Golding, Y. Kozlovsky, E. Ben-Jacob, and I.G. Ron. Continuous and discrete models of cooperation in complex bacterial colonies. *Fractals*, 7(03):235–247, 1999.

[5] N. El Khatib, S. Génieys, B. Kazmierczak, and V. Volpert. Reaction–diffusion model of atherosclerosis development. *Journal of mathematical biology*, 65(2):349–374, 2012.

[6] L.C. Evans. *Partial Differential Equations*, volume 19. American Mathematical Soc., 2010.

[7] R.A. Fisher. The wave of advance of advantageous genes. *Annals of eugenics*, 7(4):355–369, 1937.

[8] J.C. Gilkey, L.F. Jaffe, E.B. Ridgway, and G.T. Reynolds. A free calcium wave traverses the activating egg of the medaka, oryzias latipes. *The Journal of Cell Biology*, 76(2):448–466, 1978.

[9] T. Hillen and K.J. Painter. A user's guide to pde models for chemotaxis. *Journal of mathematical biology*, 58(1-2):183, 2009.

[10] D. Horstmann et al. From 1970 until present: the keller-segel model in chemotaxis and its consequences. 2003.

[11] E.F. Keller and G.M. Odell. Necessary and sufficient conditions for chemotactic bands. *Mathematical Biosciences*, 27(3-4):309–317, 1975.

[12] E.F. Keller and L.A. Segel. Initiation of slime mold aggregation viewed as an instability. *Journal of Theoretical Biology*, 26(3):399–415, 1970.

[13] E.F. Keller and L.A. Segel. Model for chemotaxis. *Journal of theoretical biology*, 30(2):225–234, 1971.

[14] E.F. Keller and L.A. Segel. Traveling bands of chemotactic bacteria: a theoretical analysis. *Journal of theoretical biology*, 30(2):235–248, 1971.

[15] I.R. Lapidus and R. Schiller. A model for traveling bands of chemotactic bacteria. *Biophysical journal*, 22(1):1–13, 1978.

[16] P.D. Lax. Hyperbolic systems of conservation laws ii. *Communications on pure and applied mathematics*, 10(4):537–566, 1957.

[17] K.W. Lee, S.E. Webb, and A.L. Miller. A wave of free cytosolic calcium traverses zebrafish eggs on activation. *Developmental biology*, 214(1):168–180, 1999.

[18] H.A. Levine, B.D. Sleeman, and M. Nilsen-Hamilton. A mathematical model for the roles of pericytes and macrophages in the initiation of angiogenesis. i. the role of protease inhibitors in preventing angiogenesis. *Mathematical biosciences*, 168(1):77–115, 2000.

[19] T. Li and Z.A. Wang. Nonlinear stability of large amplitude viscous shock waves of a generalized hyperbolic–parabolic system arising in chemotaxis. *Mathematical models and methods in applied sciences*, 20(11):1967–1998, 2010.

[20] T. Li and Z.A. Wang. Asymptotic nonlinear stability of traveling waves to conservation laws arising from chemotaxis. *Journal of Differential Equations*, 250(3):1310–1333, 2011.

[21] T. Li and Z.A. Wang. Steadily propagating waves of a chemotaxis model. *Mathematical biosciences*, 240(2):161–168, 2012.

[22] M. Luca, A. Chavez-Ross, L. Edelstein-Keshet, and A. Mogilner. Chemotactic signaling, microglia, and alzheimer's disease senile plaques: Is there a connection? *Bulletin of mathematical biology*, 65(4):693–730, 2003.

[23] R. Lui and Z.A. Wang. Traveling wave solutions from microscopic to macroscopic chemotaxis models. *Journal of mathematical biology*, 61(5):739–761, 2010.

[24] M.B.A. Mansour. Traveling wave solutions of a nonlinear reaction–diffusion–chemotaxis model for bacterial pattern formation. *Applied Mathematical Modelling*, 32(2):240–247, 2008.

[25] J.D. Murray. *Mathematical Biology. I. An Introduction*, volume 17. Springer, 2002.

[26] T. Nagai and T. Ikeda. Traveling waves in a chemotactic model. *Journal of mathematical biology*, 30(2):169–184, 1991.

[27] R. Nossal. Boundary movement of chemotactic bacterial populations. *Mathematical Biosciences*, 13(3-4):397–406, 1972.

[28] G.M. Odell and E.F. Keller. Traveling bands of chemotactic bacteria revisited. *Journal of theoretical biology*, 56(1):243–247, 1976.

[29] S.V. Rajopadhye. Some models for the propagation of bores. *Journal of Differential Equations*, 217(1):179–203, 2005.

[30] G. Rosen. Existence and nature of band solutions to generic chemotactic transport equations. *Journal of theoretical biology*, 59(1):243–246, 1976.

[31] G. Rosen and S. Baloga. On the stability of steadily propagating bands of chemotactic bacteria. *Mathematical Biosciences*, 24(3):273–279, 1975.

[32] L.A. Segel. A theoretical study of receptor mechanisms in bacterial chemotaxis. *SIAM Journal on Applied Mathematics*, 32(3):653–665, 1977.

[33] D. Serre. Systems of conservation laws: Geometric structure, oscillations and initialboundary value problems. 2000.

[34] J.A. Sherratt, E.H. Sage, and J.D. Murray. Chemical control of eukaryotic cell movement: A new model. *Journal of theoretical biology*, 162(1):23–40, 1993.

[35] B.D. Sleeman and H.A. Levine. A system of reaction diffusion equations arising in the theory of reinforced random walks. *SIAM Journal on Applied Mathematics*, 57(3):683–730, 1997.

[36] A. Stevens and H.G. Othmer. Aggregation, blowup, and collapse: the abc's of taxis in reinforced random walks. *SIAM Journal on Applied Mathematics*, 57(4):1044–1081, 1997.

[37] G. Teschl. *Ordinary differential equations and dynamical systems*, volume 140. American Mathematical Society Providence, 2012.

[38] M.J. Tindall, P.K. Maini, S.L. Porter, and J.P. Armitage. Overview of mathematical approaches used to model bacterial chemotaxis ii: bacterial populations. *Bulletin of mathematical biology*, 70(6):1570, 2008.

[39] J.J. Tyson and J.D. Murray. Cyclic amp waves during aggregation of dictyostelium amoebae. *Development*, 106(3):421–426, 1989.

[40] Z.A. Wang. Wavefront of an angiogenesis model. *Discrete Contin. Dyn. Syst.-Series B*, 17(8):2849–2860, 2012.

[41] Z.A. Wang. Mathematics of traveling waves in chemotaxisreview paper. *Discrete and Continuous Dynamical Systems Series B*, 13:601–641, 2013.

[42] Z.A. Wang and T. Hillen. Shock formation in a chemotaxis model. *Mathematical Methods in the Applied Sciences*, 31(1):45–70, 2008.

[43] Y. Yoshitmoto, T. Iwamatsu, K.I. Hirano, and Y. Hiroamoto. The wave pattern of free calcium release upon fertilization in medaka and sand dollar eggs. *Development, growth & differentiation*, 28(6):583–596, 1986.